environmental microbiology

Environmental Microbiology (2022) **24**(5), 2576–2603 doi:10.1111/1462-2920.16026

Into the darkness: the ecologies of novel 'microbial dark matter' phyla in an Antarctic lake

Timothy J. Williams, Michelle A. Allen, Pratibha Panwar and Ricardo Cavicchioli *

School of Biotechnology and Biomolecular Sciences, UNSW Sydney, Sydney, NSW, 2052, Australia.

Summary

Uncultivated microbial clades ('microbial dark matter') are inferred to play important but uncharacterized roles in nutrient cycling. Using Antarctic lake (Ace Lake, Vestfold Hills) metagenomes, 12 metagenome-assembled genomes (MAGs; 88%–100% complete) were generated for four 'dark matter' phyla: six MAGs from *Candidatus* Auribacterota (=Aureabacteria, SURF-CP-2), inferred to be hydrogen- and sulfide-producing fermentative heterotrophs, with individual MAGs encoding bacterial microcompartments (BMCs), gas vesicles, and type IV pili; one MAG (100% complete) from *Candidatus* Hinthialibacterota (=OLB16), inferred to be a facultative anaerobe capable of dissimilatory nitrate reduction to ammonia, specialized for mineralization of complex organic matter (e.g. sulfated polysaccharides), and encoding BMCs, flagella, and Tad pili; three MAGs from *Candidatus* Electryoneota (=AABM5-125-24), previously reported to include facultative anaerobes capable of dissimilatory sulfate reduction, and here inferred to perform sulfite oxidation, reverse tricarboxylic acid cycle for autotrophy, and possess numerous proteolytic enzymes; two MAGs from *Candidatus* Lernaellota (=FEN-1099), inferred to be capable of formate oxidation, amino acid fermentation, and possess numerous enzymes for protein and polysaccharide degradation. The presence of 16S rRNA gene sequences in public metagenome datasets (88%–100% identity) suggests these 'dark matter' phyla contribute to sulfur cycling, degradation of complex organic matter, ammonification and/or chemolithoautotrophic CO_2 fixation in diverse global environments.

Received 31 January, 2022; revised 18 April, 2022; accepted 20 April, 2022. *For correspondence. E-mail r.cavicchioli@unsw.edu.au.

Introduction

Uncultivated microbial clades, collectively referred to as 'microbial dark matter', include lineages that are inferred to play key roles in ecosystem formation and nutrient cycling (Rinke *et al*., 2013; Parks *et al*., 2017, 2020; Nayfach *et al*., 2020; Zamkovaya *et al*., 2021), including in Antarctica (Cavicchioli, 2015; Panwar *et al*., 2020; Ortiz *et al*., 2021; Williams *et al*., 2021a). The Antarctic lake Ace Lake is home to an extensive diversity of bacterial taxa, many of which represent higher-rank clades (class- and phylum-level) that have no cultivated representatives, and for which only a relatively small number of metagenome-assembled genomes (MAGs) are available (Ng *et al*., 2010; Lauro *et al*., 2011; Panwar *et al*., 2020; Williams *et al*., 2021a). Ace Lake is a marine-derived, 25 m deep, meromictic (permanently stratified) system located in the Vestfold Hills of East Antarctica. The water column comprises an upper oxic mixolimnion, an oxic–anoxic interface (at ~13 m) that is defined by a strong halocline and oxycline, and a stable anoxic monimolimnion (Franzmann *et al*., 1991; Rankin *et al*., 1999; Lauro *et al*., 2011; Panwar *et al*., 2020). Historically, the limnology and ecology of Ace Lake have been well studied, including being the first Antarctic system to be examined using a combination of both metagenomics and metaproteomics (Ng *et al*., 2010; Cavicchioli, 2015). Subsequent studies characterized the lake microbial community composition and function by depth (Lauro *et al*., 2011), as well as seasonal and annual dynamics (Panwar *et al*., 2020). Specific abundant members of the community, green-sulfur bacteria (GSB; *Candidatus* Chlorobium antarcticum) and 'dark matter' taxa, have also been the targeted for metagenome-based characterization (Ng *et al*., 2010; Panwar *et al*., 2021; Williams *et al*., 2021a).

In the current study we examined deeply divergent (phylum-level) uncultivated clades that were represented by Ace Lake MAGs with an estimated completeness of 88%–100%. The 'dark matter' taxa belonged to Genome Taxonomy Database (GTDB) (Chaumeil *et al*., 2019; Parks *et al*., 2020) candidate phyla SURF-CP-2 (Aureabacteria; Momper *et al*., 2017), OLB16,

AABM5-125-24, and FEN-1099. The MAGs exhibited <5% relative abundance (the majority <1%) in any of the 120 available Ace Lake metagenomes (Panwar *et al*., 2020), and were primarily from oxic–anoxic interface and anoxic monimolimnion metagenomes. The availability of previous Ace Lake physicochemical data and metagenomic assessments of the microbial community enabled us to infer ecological roles for these uncultivated bacterial phyla in Ace Lake, and interrogate public metagenome datasets to consider their possible global ecological relevance.

Results and discussion

From 12 high- and medium-quality MAGs, 10 new bacterial genera and species representing four candidate phyla were identified: six for *Candidatus* Auribacterota (SURF-CP-2; 'Aureabacteria'), one for *Candidatus* Hinthialibacterota phylum nov. (OLB16), three for *Candidatus* Electryoneota (AABM5-125-24) phylum nov. and two for *Candidatus* Lernaellota phylum nov. (FEN-1099) (Fig. 1). The MAGs were determined to represent new candidate taxa based on their average nucleotide identity (ANI) (≤77%) and amino acid identity (AAI) (≤66%) to reference strains from GTDB (Konstantinidis *et al*., 2017) and their 16S rRNA gene identity to sequences in integrated microbial genomes (IMG) isolates (<92%) and NCBI nt (<95.7%) databases (Table S2). For each MAG given below, the IMG identifier is provided, along with the MAG that we have designated as the type for the new genus and species. The metabolic capacities of each of the four phyla predicted from the MAGs of the new candidate species are described below with a view to inferring their possible ecological roles in Ace Lake.

Phylum Candidatus Auribacterota (=SURF-CP-2)

Candidate phylum SURF-CP-2 was originally based on a single MAG (SURF_26) recovered from deep terrestrial subsurface fluid of a former gold mine (Deep Mine Microbial Observatory, South Dakota, USA) (Momper *et al*., 2017). SURF-CP-2 was previously named *Candidatus* Aureabacteria, here emended to *Candidatus* Auribacterota for orthography (Trüper and Euzéby, 2009), without changing the meaning ('gold bacteria') or authorship (Momper *et al*., 2017); MAG SURF_26 is named *Ca*. Auribacter fodinae gen. et sp. nov. (Table S2). Candidate phylum SURF-CP-2 was previously described as having a 'cryptic lifestyle' on account of the absence of a suite of specific metabolic genes searched for and found to be absent on the SURF_26 MAG (Momper *et al*., 2017). Based on our interrogation of six Ace Lake MAGs (88%–98% complete; Table 1) plus the *Ca*. Auribacter fodinae MAG, we infer that *Ca*. Auribacterota are anaerobes that rely mainly on simple sugars and amino acids as heterotrophic substrates, and produce hydrogen or sulfide as fermentative byproducts.

The Ace Lake *Ca*. Auribacterota MAGs represent five different genera and species: *Ca*. Tritonobacter lacicola gen. et sp. nov. [3300035698_867 (type)]; *Ca*. Erginobacter occultus gen. et sp. nov. [3300035698_653 (type)]; *Ca*. Euphemobacter frigidus gen. et sp. nov. [3300031227_11 (type) and 3300035698_1748]; *Ca*. Ancaeobacter aquaticus gen. et sp. nov. [3300035698_1732 (type)]; *Ca*. Theseobacter exili gen. et sp. nov. [3300035698_1968 (type)] (Table S2). Collectively, these MAGs were most abundant in the Ace Lake oxic–anoxic interface and anoxic metagenomes. *Ca*. Tritonobacter lacicola and *Ca*. Euphemobacter frigidus MAGs showed up to 3.9% and 2.6% relative abundance respectively, at 23 m depth, whereas the *Ca*. Ancaeobacter aquaticus MAG showed very low abundance in metagenomes derived from the bottom waters of the lake (Table S3). The *Ca*. Euphemobacter frigidus MAGs have genes for gas vesicle production; vesicles function by providing buoyancy, enabling cells to adjust and maintain position in the water column to occupy zones with favourable growth conditions (Walsby, 1994; Youssef *et al*., 2015). The *Ca*. Erginobacter occultus MAG encodes type IV pili for attachment to surfaces, possibly cell debris and other detritus (Craig *et al*., 2019). However, whereas the *Ca*. Auribacter fodinae MAG (SURF_26) encodes flagella, none of the Ace Lake *Ca*. Auribacterota MAGs do (Table S2).

Ace Lake *Ca*. Auribacterota MAGs encode enzymes for glycolysis and gluconeogenesis pathways, including a pyrophosphate-dependent phosphofructokinase as well as ATP-dependent 6-phosphofructokinase, the former of which can reversibly function in both glycolysis and gluconeogenesis (Mertens, 1991; Kemp and Tripathi, 1993). Both enzymes are also encoded in Ace Lake MAGs from the other three candidate phyla (*Ca*. Hinthialibacterota, *Ca*. Electryoneota, *Ca*. Lernaellota), and may increase the energetic efficiency of glycolysis, especially during fermentative growth (Mertens, 1991). Among the Ace Lake *Ca*. Auribacterota, the MAG for *Ca*. Tritonobacter lacicola is exceptional in encoding a possible complete TCA cycle (Fig. 2); although there is no succinate dehydrogenase in the MAG, fumarate reductase is encoded, which is a reversible enzyme and may therefore catalyse this step (Lu and Imlay, 2017; Foo *et al*., 2020). MAGs of the other four Ace Lake species encode an incomplete TCA cycle in both the oxidative and reductive directions: genes for 2-oxoglutarate:ferredoxin oxidoreductase, succinyl-CoA synthetase, succinate dehydrogenase and fumarate reductase are all absent. Given the estimated completeness (88%–98%) of these MAGs, we regard the

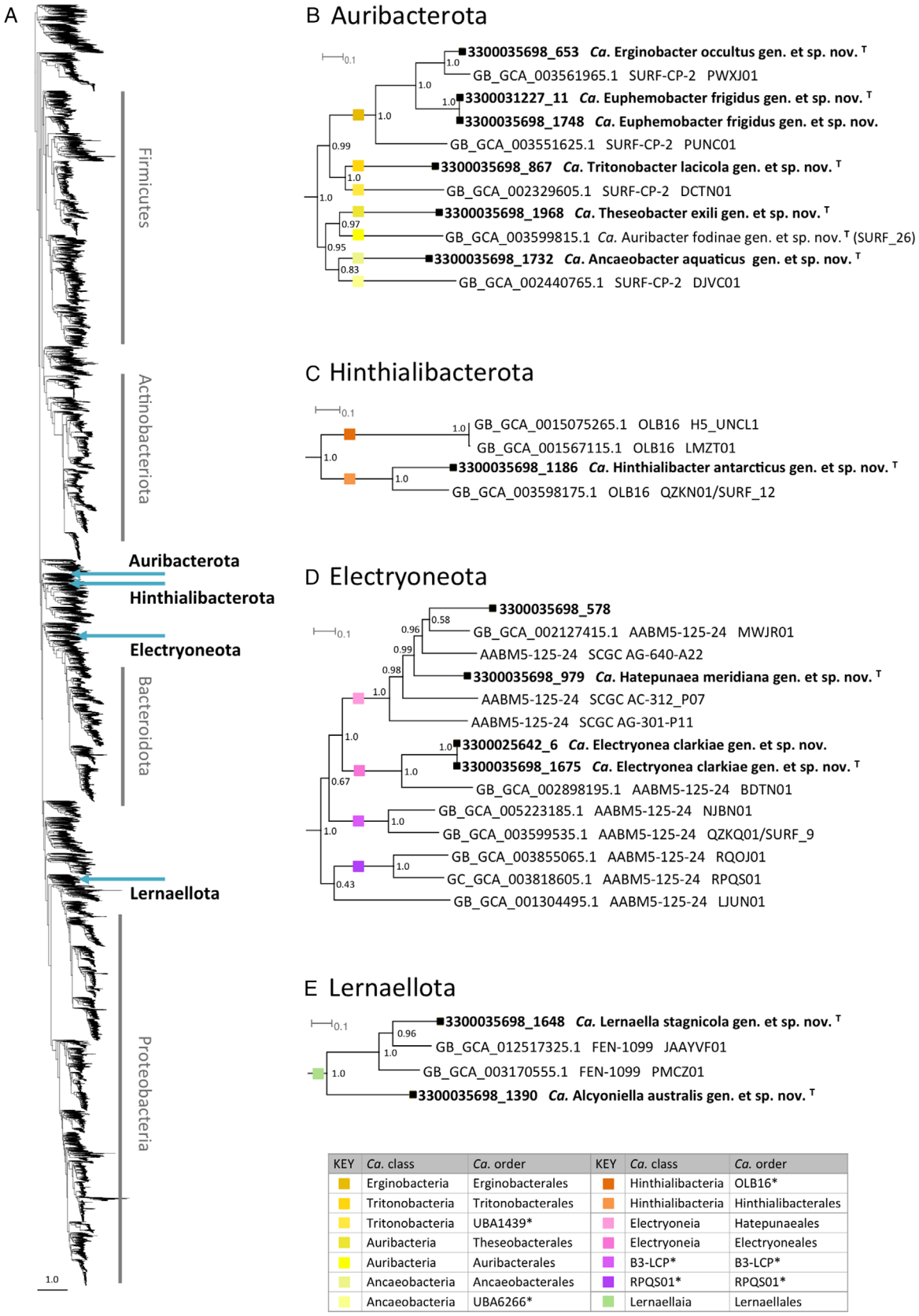

KEY	*Ca.* class	*Ca.* order	KEY	*Ca.* class	*Ca.* order
	Erginobacteria	Erginobacterales		Hinthialibacteria	OLB16*
	Tritonobacteria	Tritonobacterales		Hinthialibacteria	Hinthialibacterales
	Tritonobacteria	UBA1439*		Electryoneia	Hatepunaeales
	Auribacteria	Theseobacterales		Electryoneia	Electryoneales
	Auribacteria	Auribacterales		B3-LCP*	B3-LCP*
	Ancaeobacteria	Ancaeobacterales		RPQS01*	RPQS01*
	Ancaeobacteria	UBA6266*		Lernaellaia	Lernaellales

Fig. 1. Legend on next page.

Fig. 1. Phylogeny of four 'dark matter' phyla from Ace Lake.
A. GTDB bacterial phylogeny overview showing the placement of taxa described in this study along with major bacterial phyla. The tree was constructed from 120 single copy bacterial marker genes using the GTDB-tk *de novo* workflow with default parameters, and is rooted with the candidate phylum Patescibacteria (top left).
B–E. Zoomed-in regions of the tree showing Ace Lake MAGs from this study (given in bold, with MAG accession number preceding proposed *Candidatus* names), and neighbouring reference GTDB strains labelled with their GTDB_accession, assigned phylum and NCBI_WGS_project; (B) phylum *Candidatus* Auribacterota; (C) phylum *Candidatus* Hinthialibacterota; (D) phylum *Candidatus* Electryoneota; (E) phylum *Candidatus* Lernaellota. An additional MAG belonging to the *Candidatus* Electryoneota (D) was detected in Ace Lake in this study (3300035698_578), but due to its low completion (63%) a genus or species name was not proposed. Three sequences labelled AABM5-125-24 without a GTDB accession in (D) are single-cell microbial genomes from Youssef *et al*. (2019a) and Youssef *et al*. (2019b). Non-parametric bootstrap values are shown at nodes. ^{T}, type strain. * GTDB classes and orders in key.

incomplete TCA cycle as a likely metabolic trait, and consistent with these species having a 'horse-shoe'-type TCA pathway, as found in certain other anaerobic bacteria, where this pathway functions solely in biosynthesis (Wood *et al*., 2004; Herlemann *et al*., 2009; Marco-Urrea *et al*., 2011; Williams *et al*., 2021a). Thus, the right branch terminates at 2-oxoglutarate, the amino acceptor for ammonia assimilation and transamination reactions (see below), and the left branch allows the interconversion of oxaloacetate, malate, and fumarate (Herlemann *et al*., 2009).

Across the Ace Lake *Ca*. Auribacterota MAGs there are gene clusters that encode an array of redox-driven ion translocation systems (Complex I, Rnf, energy-converting hydrogenases, Mrp) that generate a gradient that can be used by ATP synthase to generate ATP. The majority of *Ca*. Auribacterota species encode an Rnf complex, which couples electron transfer from reduced ferredoxin to NAD^+ to generate NADH, with concomitant translocation of ions across the membrane (Tremblay *et al*., 2013). The *Ca*. Tritonobacter lacicola MAG additionally encodes a membrane-bound [NiFe] hydrogenase (Mbh) (Group 4g) (Søndergaard *et al*., 2016) and an Mrp-type Na^+/H^+ antiporter in the same gene cluster (Fig. 2). It has been proposed that Mbh transfers electrons from reduced ferredoxin to protons, thereby producing H_2 gas; doing so is likely to generate a Na^+ gradient across the cell membrane via the Mrp-type Na^+/H^+ antiporter module (Mayer and Müller, 2014; Søndergaard *et al*., 2016; Yu *et al*., 2018).

MAGs of four Ace Lake *Ca*. Auribacterota species (*Ca*. Tritonobacter lacicola, *Ca*. Euphemobacter frigidus, *Ca*. Ancaeobacter aquaticus, *Ca*. Theseobacter exili) encode a reversible, membrane-bound, energy-converting (Ech-type) hydrogenase (Group 4e). This can couple oxidation of ferredoxin (such as generated from the catabolism of sugars and amino acids) to reduction of protons (which generates H_2) and to ion translocation across the cell membrane (Sapra *et al*., 2003; Søndergaard *et al*., 2016). *Ca*. Tritonobacter lacicola additionally encodes carbon monoxide dehydrogenase (CODH), comprising the catalytic subunit (CooS) and electron transfer protein (CooF), as in *Rhodospirillum rubrum* (Kerby *et al*., 1992; Singer *et al*., 2006). We propose that CODH in *Ca*. Tritonobacter lacicola works in concert with the Ech-type hydrogenase to generate a chemiosmotic gradient by coupling CO oxidation to H_2 evolution, as reported for certain CO-oxidizing bacteria and archaea (Kerby *et al*., 1992; Schoelmerich and Müller, 2019). In the same gene cluster as the CODH genes of *Ca*. Tritonobacter lacicola are genes for acetyl-CoA synthase (ACS): the subunit (AcsB) responsible for acetyl-CoA formation via condensation of CO with a methyl group and CoA, and a corrinoid iron–sulfur complex (AcsC/AcsD) that provides the methyl group (Adam *et al*., 2018). Given that CooS (=AcsA) is reversible, one possibility is that this enzyme can also reduce CO_2 to CO for acetyl-CoA synthesis, as part of a CODH–ACS complex. This raises the possibility that CO_2 could be fixed to generate acetyl-CoA, which could be further carboxylated to pyruvate using pyruvate:ferredoxin oxidoreductase (POR) (Ragsdale and Pierce, 2008). Thus, *Ca*. Tritonobacter lacicola may have a reversible CODH that has distinct metabolic functions according to the identity of the enzyme it associates with: CO oxidized to drive proton translocation when CODH acts in concert with Ech hydrogenase; or CO_2 reduced to CO for acetyl-CoA synthesis when CODH acts as part of a CODH–ACS complex.

Ca. Erginobacter occultus and *Ca*. Euphemobacter frigidus MAGs also encode components of ACS (AcsB, AcsC/AcsD), but no CooS/AcsA homologue; thus, in both species the ACS could be used to cleave acetyl-CoA to generate a methyl group for methionine synthesis, as in *Dehalococcoides mccartyi* (Zhuang *et al*., 2014). No *Ca*. Auribacterota MAG encodes a complete methyl branch of the Wood–Ljungdahl pathway, although a truncated version is encoded in the *Ca*. Tritonobacter lacicola MAG, comprising formate-tetrahydrofolate [THF] synthase [Fhs] and bifunctional methylene-THF dehydrogenase/methenyl-THF cyclohydrolase [FolD]), as in *D. mccartyi*. In *D. mccartyi*, this truncated Wood–Ljungdahl pathway is used for the conversion of glycine to serine, by sourcing the methylene group from exogenous formate (Zhuang *et al*., 2014). Overall, Ace Lake *Ca*. Auribacterota MAGs possess genes that indicate diverse approaches to one-carbon metabolism.

Table 1. Summary of the physiological and metabolic traits inferred from six Ace Lake MAGs of phylum *Candidatus* Auribacterota (=Aureabacteria).

***Candidatus* Tritonobacter lacicola** gen. et sp. nov.
Genus named after the Greek demi-god Triton, a son of the sea god Poseidon who inhabited a salt lake also called Triton; species name means 'lake-dweller'
3300035698_867 (type): 92% complete, 2.2% contamination
Highest abundance: 3.9% (23 m, anoxic zone)
Glycolysis and gluconeogenesis (includes both ATP-dependent and PP_i-dependent 6-phosphofructokinase; both NAD- and ferredoxin-dependent glyceraldehyde 3-phosphate dehydrogenase)
TCA cycle (oxidative) [includes citrate *(Si)*-synthase]
Pentose phosphate pathway (non-oxidative only)
F-type ATP synthase
Ion-translocating ferredoxin:NAD+ oxidoreductase Rnf complex
Membrane-bound [NiFe] hydrogenase (Mbh) (Group 4 g) + Mrp-type Na^+/H^+ antiporter module
Ech-type membrane-bound [NiFe] hydrogenase (Group 4e)
Carbon monoxide oxidation (coupled to Ech-type hydrogenase) and reduction
Partial Wood–Ljungdahl pathway
Sulfhydrogenase ([NiFe] hydrogenase [Group 3b]/sulfur reductase), cytoplasmic
Glycoside hydrolases: 3 (two with signal peptide)
Trehalose and glycogen synthesis
Sulfatases: 4 (three with signal peptide)
Proteases/peptidases: seven (none with signal peptide)
Fermentation of BCAA
BMC (involved in DNA degradation/aldehyde oxidation)
Degradation of diaminopropionate, glycolate alcohols
Synthesis of all 20 amino acids required for protein synthesis
ABC transporters: sugars, peptides, osmoprotectants, tungstate
Other transporters: amino acids, nucleosides, nucleobases, phosphate, Fe(II), Zn, Mg
Desulfoferrodoxin, hydroxylamine reductase
***Candidatus* Erginobacter occultus** gen. et sp. nov.
Genus named after Erginus the Argonaut, a son of the sea god Poseidon, in reference to both maritime exploration and to the marine origin of Ace Lake; species name means 'hidden'
3300035698_653 (type): 95% complete, 2.2% contamination
Highest abundance: 0.16% (24 m, anoxic zone)
Glycolysis and gluconeogenesis (includes both ATP-dependent and PP_i-dependent 6-phosphofructokinase)
Incomplete TCA cycle [includes citrate (*Re*)-synthase]
Pentose phosphate pathway (oxidative, non-oxidative)
V-type ATP synthase
Ion-translocating ferredoxin:NAD+ oxidoreductase Rnf complex
Sulfhydrogenase ([NiFe] hydrogenase [Group 3b]/sulfur reductase), cytoplasmic
[FeFe] hydrogenase, bifurcating (Group A3), cytoplasmic
Partial Wood–Ljungdahl pathway, CO reduction to acetyl-CoA.
Glycoside hydrolases: 7 (two with signal peptide)
Trehalose and glycogen synthesis
Sulfatases: 8 (seven with signal peptide)
Proteases/peptidases: 10 (nine with signal peptide)
Fermentation of BCAA and aromatic amino acids
Degradation of lactate, diaminopropionate
BMC (involved in DNA degradation/aldehyde oxidation)
Acetyl-CoA to acetate, with ATP generation by substrate-level phosphorylation
Synthesis of almost all 20 amino acids required for protein synthesis
ABC transporters: sugars, peptides, phosphate, cobalamin, tungstate
Other transporters: amino acids, carboxylic acids, nucleosides, nucleobases, phosphate, Fe(II), Mg
Type IV pili
***Candidatus* Euphemobacter frigidus** gen. et sp. nov.
Genus named after Euphemus the Argonaut, a son of the sea god Poseidon; species name means 'cold'
3300031227_11 (type): 95% complete, 4.3% contamination
3300035698_1748: 96.8% complete, 5.4% contamination
Highest abundance: 2.6% (23 m, anoxic zone)
Glycolysis and gluconeogenesis (includes both ATP-dependent and PP_i-dependent 6-phosphofructokinase; both NAD- and ferredoxin-dependent glyceraldehyde 3-phosphate dehydrogenase)
Incomplete TCA cycle [includes citrate (*Re*)-synthase]
Pentose phosphate pathway (oxidative, non-oxidative)
V-type ATP synthase
Ion-translocating ferredoxin:NAD+ oxidoreductase Rnf complex
Ech-type membrane-bound [NiFe] hydrogenase (Group 4e)
Sulfhydrogenase ([NiFe] hydrogenase [Group 3b]/sulfur reductase), cytoplasmic
Partial Wood–Ljungdahl pathway

(Continues)

Table 1. Continued

Glycoside hydrolases: 6 (three with signal peptide)
Trehalose and glycogen synthesis
Sulfatase: 1 (has signal peptide)
Proteases/peptidases: 910 (five with signal peptide)
Fermentation of BCAA and aromatic amino acids
BMC (involved in DNA degradation/aldehyde oxidation)
Degradation of lactate, diaminopropionate
Acetyl-CoA to acetate, with ATP generation by substrate-level phosphorylation
Synthesis of almost all 20 amino acids required for protein synthesis
ABC transporters: sugars, peptides, BCAA, cobalamin, molybdate, tungstate
Other transporters: sugars, amino acids, nucleosides, nucleobases, phosphate, Fe(II), Zn, Mg, Co
Desulfoferrodoxin
Gas vesicles
Type IV pili
***Candidatus* Ancaeobacter aquaticus** gen. et sp. nov.
Genus named after Ancaeus the Argonaut, a son of the sea god Poseidon; species name means 'found in the water'
3300035698_1732 (type): 98% complete, 2.2% contamination
Highest abundance: 1.6% (18 m, anoxic zone)
Glycolysis and gluconeogenesis (includes both ATP-dependent and PP_i-dependent 6-phosphofructokinase)
Incomplete TCA cycle [includes citrate (*Re*)-synthase]
Pentose phosphate pathway (oxidative, non-oxidative)
NADH-quinone oxidoreductase (complex I)
V-type ATP synthase
Ech-type membrane-bound [NiFe] hydrogenase (Group 4e)
Sulfhydrogenase ([NiFe] hydrogenase [Group 3b]/sulfur reductase), cytoplasmic
Glycoside hydrolases: 9 (none with signal peptide)
Trehalose and glycogen synthesis
Proteases/peptidases: 7 (none with signal peptide)
Degradation of glycerol
Fermentation of BCAA
Synthesis of almost all 20 amino acids required for protein synthesis
ABC transporters: sugars, peptides, cobalamin, Ni, Mn
Other transporters: sugars, ammonia, amino acids, nucleosides, nucleobases, phosphate, Fe(II), Zn, Mg, Co
Desulfoferrodoxin, hydroxylamine reductase
***Candidatus* Theseobacter exili** gen. et sp. nov.
Genus named after Theseus the Argonaut, a son of the sea god Poseidon, as for above; species name means 'exile' or 'isolation'
3300035698_1968 (type): 88% complete, 3.2% contamination
Highest abundance: 0.15% (23 m, anoxic zone)
Glycolysis and gluconeogenesis (includes PP_i-dependent 6-phosphofructokinase)
Incomplete TCA cycle
Pentose phosphate pathway (oxidative, non-oxidative)
F-type and V-type ATP synthases
Ion-translocating ferredoxin:NAD+ oxidoreductase Rnf complex
Ech-type, membrane-bound [NiFe] hydrogenase (Group 4e)
Sulfhydrogenase ([NiFe] hydrogenase [Group 3b]/sulfur reductase), cytoplasmic
Glycoside hydrolases: 8 (one with signal peptide)
Trehalose and glycogen synthesis
Sulfatases: 4 (all with signal peptide)
Proteases/peptidases: 11 (six with signal peptide)
Degradation of dihydroxyacetone, alcohols
Synthesis of almost all 20 amino acids required for protein synthesis
Polyphosphate synthesis
ABC transporters: sugars, peptides, BCAA, cobalamin, Zn/Mn, molybdate
Other transporters: sugars, nucleobases, phosphate, sulfate, Fe(II), Zn, Mg
Desulfoferrodoxin, hydroxylamine reductase

The complete etymologies of genera and species are given in Table S2. A summary of inferred traits for the deep terrestrial subsurface fluid *Candidatus* Auribacter fodinae gen. et sp. nov. is also provided in Table S2.

The *Ca*. Erginobacter occultus MAG encodes a [FeFe] hydrogenase (Group A3) that might act during fermentation as an H_2-evolving, confurcating hydrogenase from reduced ferredoxin and NADH; although it could also serve in the opposite direction to oxidize H_2 as an energy source through the bifurcation of electrons to ferredoxin and NAD^+ (Poudel *et al*., 2016; Søndergaard *et al*., 2016). A bifunctional sulfhydrogenase ([NiFe] hydrogenase/sulfur reductase) is encoded in MAGs of all Ace Lake *Ca*. Auribacterota species. This tetrameric sulfhydrogenase allows excess reductant generated during fermentation to be

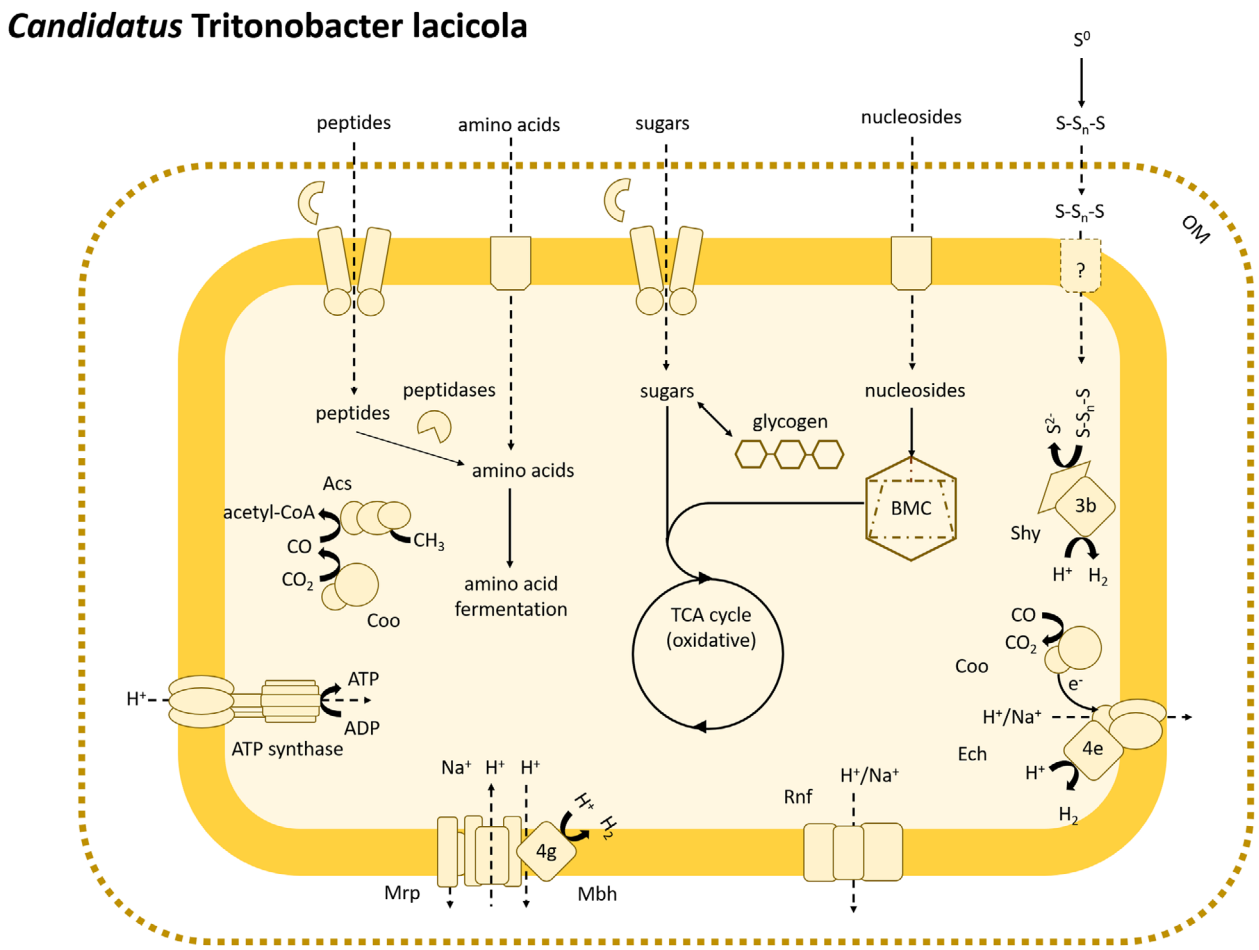

Fig. 2. Metabolic capacities of *Candidatus* Tritonobacter lacicola (candidate phylum Auribacterota) as inferred from MAG sequences. Elemental sulfur (S_0) is shown entering the cell as soluble polysulfide ($S\text{-}S_n\text{-}S$), but the mechanism for transport of $S\text{-}S_n\text{-}S$ into the cytoplasm is not known. 3b, [NiFe] hydrogenase Group 3b; 4e, [NiFe] hydrogenase Group 4e; 4g, [NiFe] hydrogenase Group 4g; Acs, acetyl-CoA synthase; BMC, bacterial microcompartment; CoA, coenzyme A; Coo, carbon monoxide dehydrogenase; Ech, energy-converting hydrogenase; Mbh, membrane-bound [NiFe] hydrogenase; Mrp, Mrp-type Na^+/H^+ antiporter; OM, outer membrane; Rnf, ion-translocating ferredoxin:NAD^+ oxidoreductase complex; Shy, sulfhydrogenase; TCA, tricarboxylic acid.

disposed of as H_2 and sulfide respectively (Ma *et al*., 1993; Silva *et al*., 1999; Ma *et al*., 2000).

The Ace Lake *Ca*. Auribacterota MAGs encode relatively few glycoside hydrolases for the depolymerization of polysaccharides and glycoconjugates. Substrates such as simple sugars, peptides and free amino acids would be imported directly from the environment by specific transporters. Amino acids could be procured through digestion of peptides; numerous proteases and peptidases are encoded in these MAGs. A pathway for the fermentation of branched-chain amino acids (BCAA) is encoded in MAGs of four Ace Lake species, and three encode a pathway for aromatic amino acid fermentation. For the former, BCAA aminotransferase converts BCAA to branched-chain oxoacids, using 2-oxoglutarate as the amino group acceptor, with this transamination also producing glutamate; branched-chain oxoacids can then be oxidatively decarboxylated by ketoisovalerate oxidoreductase (VOR) to generate reduced ferredoxin (Schut *et al*., 2001). Similarly, aromatic amino acid aminotransferase converts aromatic amino acids to arylpyruvates; arylpyruvates are oxidatively decarboxylated by indolepyruvate oxidoreductase (IOR) to generate reduced ferredoxin (Mai and Adams, 1994). The glutamate generated from the initial transaminations can be recycled back to 2-oxoglutarate using glutamate dehydrogenase with the concomitant reduction of NAD^+ or $NADP^+$ (Daebeler *et al*., 2018).

MAGs of two species (*Ca*. Tritonobacter lacicola, *Ca*. Erginobacter occultus) encode shell and vertex proteins for the construction of BMCs. BMCs have diverse metabolic functions across the domain Bacteria (Kennedy *et al*., 2021; Sutter *et al*., 2021); we predict that those encoded in these *Ca*. Auribacterota are catabolic BMCs

used for DNA degradation. Deoxyribose-phosphate aldolase converts 2-deoxy-D-ribose to glyceraldehyde-3-phosphate (a glycolytic intermediate) and acetaldehyde, the latter of which is toxic. Multiple aldehyde:ferredoxin oxidoreductases are encoded in both species and may function in the oxidation of toxic aldehydes, generating reduced ferredoxin and acetate, and acetaldehyde may be processed by acetaldehyde dehydrogenase to acetyl-CoA (Sutter *et al*., 2021).

Phylum Candidatus Hinthialibacterota (=OLB16)

Formerly included in phylum *Ca*. Omnitrophota within the 'Planctomycetes–Verrucomicrobia–Chlamydiae' superphylum, OLB16 is a recently recognized bacterial phylum named after OLB16, a MAG recovered from a partial-nitritation anammox reactor (Liu *et al*., 2020). Another MAG from phylum OLB16 (SURF_12) was recovered from same deep terrestrial subsurface fluid as SURF_26 (Momper *et al*., 2017). SURF_12 was predicted to be capable of nitrate reduction, sulfite oxidation, methane oxidation, and carbon fixation via the Wood–Ljungdahl pathway (Momper *et al*., 2017). Two further OLB16 MAGs from the same subsurface fluids were predicted to be fermentative heterotrophs capable of sulfur oxidation/reduction, metal reduction, and hydrogen oxidation/generation (Momper *et al*., 2021).

From Ace Lake, a single OLB16 MAG (3300035698_1186; 100% complete) was identified and is here designated the type MAG for *Ca*. Hinthialibacter antarcticus gen. et sp. nov., with the OLB16 candidate phylum named *Ca*. Hinthialibacterota phylum nov. (Table 2; Table S2). Very few of the metabolic abilities inferred from the deep terrestrial subsurface fluid OLB16 MAGs were encoded in the *Ca*. Hinthialibacter antarcticus MAG, suggesting that the metabolism of the Ace Lake representative is distinct.

The *Ca*. Hinthialibacter antarcticus MAG had the highest relative abundance (0.9%) in the oxic–anoxic interface of Ace Lake (where *Ca*. Chlorobium antarcticum dominates; Panwar *et al*., 2020; Panwar *et al*., 2021), as well as being detected in the oxic zone above and anoxic zone below the interface (Table S3). Genes for cytochrome *c* oxidase complex are consistent with the capacity for aerobic respiration. We predict *Ca*. Hinthialibacter antarcticus to be a facultative anaerobe capable of dissimilatory nitrate reduction to ammonia (DNRA), based on genes for respiratory nitrate reductase (NarGH) and nitrite reductase (cytochrome *c*-552) (NrfAH) (Einsle *et al*., 1999) (Fig. 3). Nitrate and nitrite levels are at low concentrations in the oxygenated layers of Ace Lake (<0.4 mM) (Rankin *et al*., 1999), and not detected in the anoxic zone, which likely limits the capacity for DNRA below the interface. Under anoxic conditions, *Ca*. Hinthialibacter antarcticus is inferred to also use fermentation: two bidirectional cytoplasmic [NiFe] hydrogenases are encoded in this MAG (Table 2), which would facilitate fermentative growth, as well as allow H_2 to be used as an energy source (Heim *et al*., 1998; Kaster *et al*., 2011; Greening *et al*., 2016).

Based on the numerous GH genes from many GH families, *Ca*. Hinthialibacter antarcticus is predicted to have the capacity to degrade a diverse array of polysaccharides, including those derived from the cell walls of algae. The MAG also encodes abundant proteases and peptidases. Thus, we infer that this bacterium is capable of obtaining substrates from the degradation of biopolymers. As well as flagella for swimming motility, *Ca*. Hinthialibacter antarcticus encodes Tad (tight adherence) pili (Giltner

Table 2. Summary of the physiological and metabolic traits inferred from the Ace Lake MAG of phylum *Candidatus* Hinthialibacterota phylum nov.

***Candidatus* Hinthialibacter antarcticus** gen. et sp. nov.
Genus named after the Etruscan word *hinthial*, meaning 'shade' or 'of the underworld'; the species name means 'southern'
3300035698_1186 (type): 100% complete, 0% contamination
Highest abundance: 0.9% (13 m, oxic–anoxic interface)
Glycolysis and gluconeogenesis (includes both ATP-dependent and PP_i-dependent 6-phosphofructokinase)
TCA cycle (oxidative) [includes citrate (*Si*)-synthase]
Pentose phosphate pathway (non-oxidative)
Aerobic respiration: cytochrome *c* oxidase complex
Anaerobic respiration: dissimilatory nitrate reductase and dissimilatory nitrite reductase (cytochrome *c*-552); nitrate reduced to ammonia via nitrite
NADH-quinone oxidoreductase (complex I)
F-type ATP synthase
Cytoplasmic [NiFe] hydrogenases: NAD-coupled (Group 3d); bifurcating, heterodisulfide reductase-linked (Group 3c): used for H_2 oxidation and/or fermentation
Assimilatory sulfate reduction
NAD(P) transhydrogenase
Glycoside hydrolases and pectinolytic enzymes: 42 (34 with signal peptide)
Sulfatases: 39 (34 with signal peptide)
Degradation of fucose, rhamnose, xylose, gluconate/glucuronate, phosphonate, alcohols
Glycogen synthesis
Fermentation of aromatic amino acids
BMC (involved in fucose, rhamnose and phosphonate degradation/ aldehyde oxidation)
Acetyl-CoA to acetate, with ATP generation by substrate-level phosphorylation
Proteases/peptidases: 14 (five with signal peptide)
Polyphosphate synthesis
ABC transporters: sugars, peptides, BCAA, osmoprotectants, nucleosides, cobalamin, Fe(III), Mn, Zn, Co/Ni, molybdate
Other transporters: sugars, ammonia, amino acids, nucleosides, carboxylates, gluconates, phosphate, sulfate, Fe(II), Zn, Mg
Catalase, catalase-peroxidase, superoxide dismutase, hydroxylamine reductase
Flagella
Tight adherence (Tad) pili

The complete etymologies of the genus and species are given in Table S2.

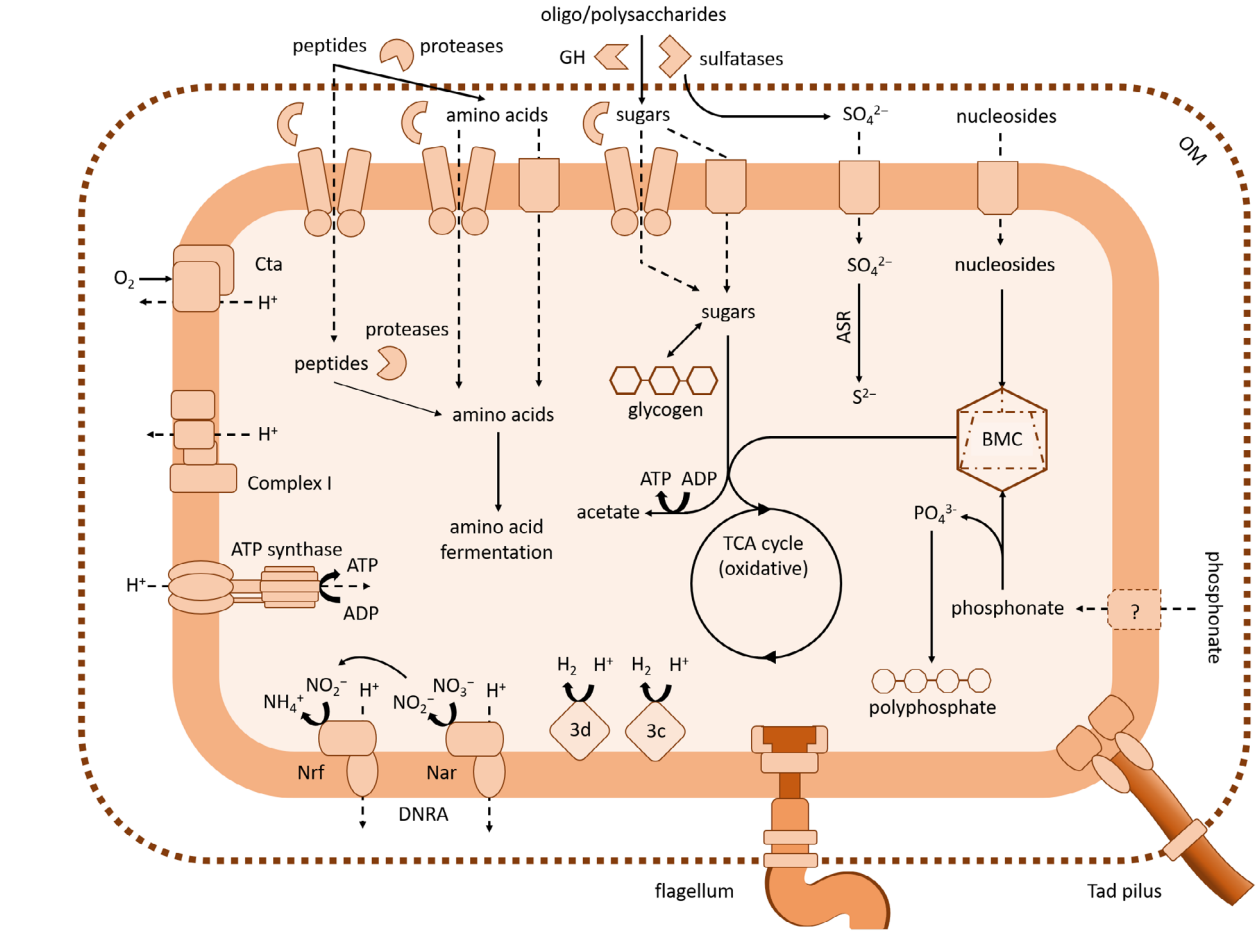

Fig. 3. Metabolic capacities of *Candidatus* Hinthialibacter antarcticus (candidate phylum Hinthialibacterota) as inferred from MAG sequences. Oligo/polysaccharides include both sulfated and non-sulfated oligo/polysaccharides. The transporter by which phosphonate enters the cytoplasm is not known. 3c, [NiFe] hydrogenase Group 3c; 3d, [NiFe] hydrogenase Group 3d; ASR, assimilatory sulfate reduction; BMC, bacterial microcompartment; Cta, cytochrome *c* oxidase; DNRA, dissimilatory nitrate reduction to ammonia; GH, glycoside hydrolases; Nar, respiratory nitrate reductase; Nrf, nitrite reductase (cytochrome *c*-552); OM, outer membrane; Tad, tight adherence; TCA, tricarboxylic acid.

et al., 2012), which could possibly be utilized for attachment to cell debris and other detritus. Potential pectinolytic enzymes (e.g. glucuronyl hydrolase, polygalacturonan lyase, polygalacturonase), all of which include N-terminal signal peptides (suggesting they act extracytoplasmically), may generate oligosaccharides and hexuronates from pectin for further catabolism. Other polysaccharides that *Ca*. Hinthialibacter antarcticus could degrade include sulfated polysaccharides such as fucoidans. Fucoidans are predominantly composed of fucose with a variable composition of other monosaccharides such as glucose, rhamnose, mannose, and xylose (Ale *et al*., 2011). Fucosidases, rhamnosidases, and xylosidases are also encoded (the majority with signal peptides) for the release of fucose, rhamnose, and xylose, respectively, from polysaccharides, as are enzymes for their subsequent catabolism (Bunesova *et al*., 2016). Fucoidan digestion is facilitated by sulfatases, which catalyse the hydrolytic cleavage of sulfate esters to remove the sulfate groups (Wegner *et al*., 2013). *Ca*. Hinthialibacter antarcticus encodes 39 sulfatases; the majority of these (34) include N-terminal signal peptides, which suggest a periplasmic or extracellular location, as predicted for sulfatases involved in sulfated polysaccharide degradation by other bacteria (e.g. Reisky *et al*., 2019; van Vliet *et al*., 2019). Collectively, these sulfatases from *Ca*. Hinthialibacter antarcticus appear to be involved in the degradation of disparate substrates, with certain sulfatases showing the highest sequence identities to sulfatases that target sulfated algal polysaccharides (Reisky *et al*., 2019), whereas others show the highest sequence identities to glycosaminoglycan sulfatases (Ulmer *et al*., 2014).

The *Ca*. Hinthialibacter antarcticus MAG encodes shell and vertex proteins for BMCs, which could be used to contain lactaldehyde, a toxic product of fucose and rhamnose degradation (Orellana *et al*., 2021) that can be converted to lactate by lactaldehyde dehydrogenase. BMCs may also be associated with phosphonate degradation, with the MAG encoding the two enzymes (2-aminoethylphosphonate-pyruvate transaminase, PhnW; phosphonoacetaldehyde hydrolase, PhnX) for the degradation of the most common biogenic phosphonate, 2-aminoethylphosphonate, to alanine, phosphate, and acetaldehyde, with the latter converted by acetaldehyde dehydrogenase to acetyl-CoA in BMCs (Zangelmi *et al*., 2021). Also encoded is the ammonia-lyase for conversion of another naturally occurring phosphonate, (R)-1-hydroxy-2-aminoethylphosphonate, to phosphonoacetaldehyde, which can then be catabolized by PhnX (Zangelmi *et al*., 2021). Thus, phosphonates have the potential to be used by *Ca*. Hinthialibacter antarcticus as a source of phosphate, nitrogen, and perhaps energy, if acetyl-CoA is used to generate ATP by substrate-level phosphorylation by the sequential action of acetate kinase and phosphate acetyltransferase.

Phylum Candidatus Electryoneota (=AABM5-125-24)

Candidate phylum AABM5-125-24 belongs to the FCB ('Fibrobacteres-Chlorobi-Bacteroidetes') superphylum, and is here named *Candidatus* Electryoneota phylum nov. Three Ace Lake MAGs (90%–97% complete) represented two new genera and species of this phylum: *Ca*. Electryonea clarkiae gen. et sp. nov. [3300035698_1675 (type) and 3300025642_6]; *Ca*. Hatepunaea meridiana gen. et sp. nov. [3300035698_979 (type)] (Table 3). A third genus represented by a fourth MAG had low completion (3300035698_578; 63%), and revealed comparatively little regarding its potential metabolic abilities (Table S1). We interpret *Ca*. Electryonea clarkiae and *Ca*. Hatepunaea meridiana to be facultative anaerobes, capable of aerobic respiration using high O_2 affinity enzymes and anaerobic respiration using dissimilatory sulfate reduction (DSR), as previously inferred for other MAGs (from aquatic sediment or oceanic samples) assigned to candidate phylum *Ca*. Electryoneota (Youssef *et al*., 2019a). The high O_2 affinity enzymes cytochrome *bd* respiratory O_2 reductase (Borisov *et al*., 2011) and cytochrome c oxidase *cbb3*-type (Buschmann *et al*., 2010) are encoded in the *Ca*. Electryonea clarkiae MAGs (Fig. 4), whereas only the former was detected in the *Ca*. Hatepunaea meridiana MAG. Both have a full suite of genes required for DSR: sulfate adenylyltransferase (Sat), adenylylsulfate reductase (AprAB), dissimilatory-type sulfite reductase (DsvAB), and quinone-modifying oxidoreductase complex (QmoABC) (Duarte *et al*., 2016; Youssef *et al*., 2019a). *Ca*. Electryonea clarkiae and *Ca*. Hatepunaea meridiana MAGs had the highest relative abundances in the anoxic zone, at 1.2% (14 m depth) and 0.6% (18 m depth), respectively (Table S3). These facultative aerobes may use high O_2 affinity respiratory enzymes within the steep oxycline of the oxic–anoxic interface (Rankin *et al*., 1999; Lauro *et al*., 2011); however, unlike *Ca*. Electryonea clarkiae, *Ca*. Hatepunaea meridiana was barely detected in the oxic–anoxic interface metagenomes (Table S3). Sulfate, required for respiration by DSR, is abundant in the oxic–anoxic interface of Ace Lake, but increasingly limiting with depth in the anoxic zone (Burton and Barker, 1979; Franzmann *et al*., 1991; Rankin *et al*., 1999) (Fig. S1).

A number of previously unreported metabolic traits for phylum *Ca*. Electryoneota were apparent from examination of the Ace Lake MAGs. The *Ca*. Electryonea clarkiae and *Ca*. Hatepunaea meridiana MAGs possess gene clusters for membrane-bound Complex Iron–Sulfur Molybdoenzyme (CISM) complexes (Schoepp-Cothenet *et al*., 2012). Typical of these complexes, each comprises three subunits: a molybdopterin-binding catalytic subunit, an electron transfer subunit, and a membrane anchor subunit involved in the transfer of electrons from the quinone pool (Kadnikov *et al*., 2013) that has also been proposed to carry out proton translocation (Jormakka *et al*., 2008; Marreiros *et al*., 2016; Calisto and Pereira, 2021). *Ca*. Electryonea clarkiae encodes two CISM clusters, whereas *Ca*. Hatepunaea meridiana encodes one. Phylogenetic analysis of the catalytic subunits of each of these revealed that both *Ca*. Electryonea clarkiae and *Ca*. Hatepunaea meridiana encode a sulfite dehydrogenase (SoeABC; SoeA corresponds to the catalytic subunit), and that *Ca*. Electryonea clarkiae additionally encodes a possible thiosulfate reductase (see below) (Fig. 5). Sulfite dehydrogenase is responsible for the oxidation of sulfite in the cytoplasm, as in *Allochromatium vinosum* (Dahl *et al*., 2013). Thus, we posit that *Ca*. Electryoneota possess two possible routes for sulfite detoxification: reduction of sulfite by DsvAB, as the terminal step of DSR; or oxidation by SoeABC, which as well as being energetically favourable (Simon and Kroneck, 2013), allows sulfate to be regenerated.

Ca. Electryonea clarkiae MAGs encode a second CISM complex, for which the catalytic subunit has a signal peptide (Tat) for a periplasmic orientation. Phylogenetic analysis of this catalytic subunit recovered it within a cluster that includes the catalytic subunits of known thiosulfate reductases (PhsA) from *Salmonella enterica* (Clark and Barrett, 1987; Hinsley and Berks, 2002), *Shewanella oneidensis* (Burns and DiChristina, 2009), and *Desulfovibrio vulgaris* (Aketagawa *et al*., 1985), and polysulfide reductase (PsrA) from *Wolinella succinogenes* (Krafft *et al*., 1992) (Fig. 5). Within this PhsA/PsrA cluster, the homologue in the *Ca*. Electryonea clarkiae MAG showed the highest sequence identity

Table 3. Summary of the physiological and metabolic traits inferred from three Ace Lake MAGs of phylum *Candidatus* Electryoneota phylum nov.

***Candidatus* Electryonea clarkiae** gen. et sp. nov.
Genus named after the Greek demi-goddess Electryone, who presides over awakening from sleep; species named in honour of marine biologist Eugenie Clark
3300035698_1675 (type): 97% complete, 1.1% contamination
3300025642_6: 90% complete, 6.1% contamination
Highest abundance: 1.2% (14 m, anoxic zone)
Glycolysis, gluconeogenesis (includes both ATP-dependent and PP_i-dependent 6-phosphofructokinase)
TCA cycle (oxidative) [includes citrate (*Si*)-synthase]
TCA cycle (reductive) (includes fumarate reductase, reversible citrate synthase)
Pentose phosphate pathway (non-oxidative)
Aerobic respiration: cytochrome *bd* respiratory O_2 reductase, and cytochrome *c* oxidase *cbb3*-type; both high O_2 affinity
Anaerobic respiration: dissimilatory sulfate reduction
Sulfite oxidation
Thiosulfate reduction
NADH-quinone oxidoreductase (complex I)
F-type ATP synthase
Ferredoxin:NAD+ oxidoreductase Rnf complex
NAD(P) transhydrogenase
Cytoplasmic [FeFe] hydrogenase, bifurcating (Group A3): used for H_2 oxidation (such as to drive reductive TCA cycle)
Glycoside hydrolases: 3 (none with signal peptide)
Glycogen synthesis
Acetyl-CoA to acetate, with ATP generation by substrate-level phosphorylation
Proteases/peptidases: 38 (25 with signal peptide)
Fermentation of BCAA and aromatic amino acids
Degradation of aspartate, proline, *trans*-4-hydroxy-L-proline, methionine, histidine, tryptophan, diaminopropionate, glycerol, alcohols
Poly-γ-glutamate synthesis
Synthesis of glutamate, glutamine, aspartate, asparagine, alanine, serine, glycine, methionine, cysteine, lysine, BCAA
ABC transporters: sugars, peptides, phosphate, molybdate, Zn, Mn
Other transporters: sugars, peptides, amino acids, nucleosides, carboxylates, phosphate, sulfate, Fe (II), Zn, Mn, Mg
Bacillithiol synthesis
Catalase, desulfoferrodoxin
Flagella
***Candidatus* Hatepunaea meridiana** gen. et sp. nov.
Genus named after Hatepuna, a Hattian water deity and daughter of a sea god; species name means 'of the south'
3300035698_979 (type): 95% complete, 0% contamination
Highest abundance: 0.6% (18 m, anoxic zone)
Glycolysis, gluconeogenesis (includes PP_i-dependent 6-phosphofructokinase)
TCA cycle (oxidative) [includes citrate (*Si*)-synthase]
TCA cycle (reductive) (includes fumarate reductase, reversible citrate synthase)
Pentose phosphate pathway (non-oxidative)
Aerobic respiration: cytochrome *bd* respiratory O_2 reductase; high O_2 affinity
Anaerobic respiration: dissimilatory sulfate reduction
Sulfite oxidation
NADH-quinone oxidoreductase (complex I)
F-type ATP synthase
Ferredoxin:NAD+ oxidoreductase Rnf complex
Glycoside hydrolases: 2 (one with signal peptide)
Glycogen synthesis
Acetyl-CoA to acetate, with ATP generation by substrate-level phosphorylation
Proteases/peptidases: 27 (16 with signal peptide)
Fermentation of BCAA and aromatic amino acids
Degradation of aspartate, methionine, histidine, tryptophan
Poly-γ-glutamate synthesis
Synthesis of glutamate, glutamine, aspartate, asparagine, alanine, serine, glycine, methionine, cysteine, lysine, BCAA
ABC transporters: peptides, Zn
Other transporters: peptides, amino acids, carboxylates, phosphate, sulfate, Fe (II), Zn, Mg
Bacillithiol synthesis
Catalase, desulfoferrodoxin
Flagella? (flagellar genes are encoded, but not flagellin genes)

The complete etymologies of genera and species are given in Table S2.

(57%) and the closest phylogenetic relationship (Fig. 5) to the PhsA/PsrA subunit of a putative thiosulfate/polysulfide reductase (Phs/Psr) in *Caldithrix abyssi* (Kublanov *et al*., 2017). Previous work found that thiosulfate stimulated fermentative growth of *C. abyssi* when peptone was supplied as a growth substrate, and led to sulfide being produced; however, thiosulfate did not support *C. abyssi* growth by respiration using acetate

Candidatus Electryonea clarkiae

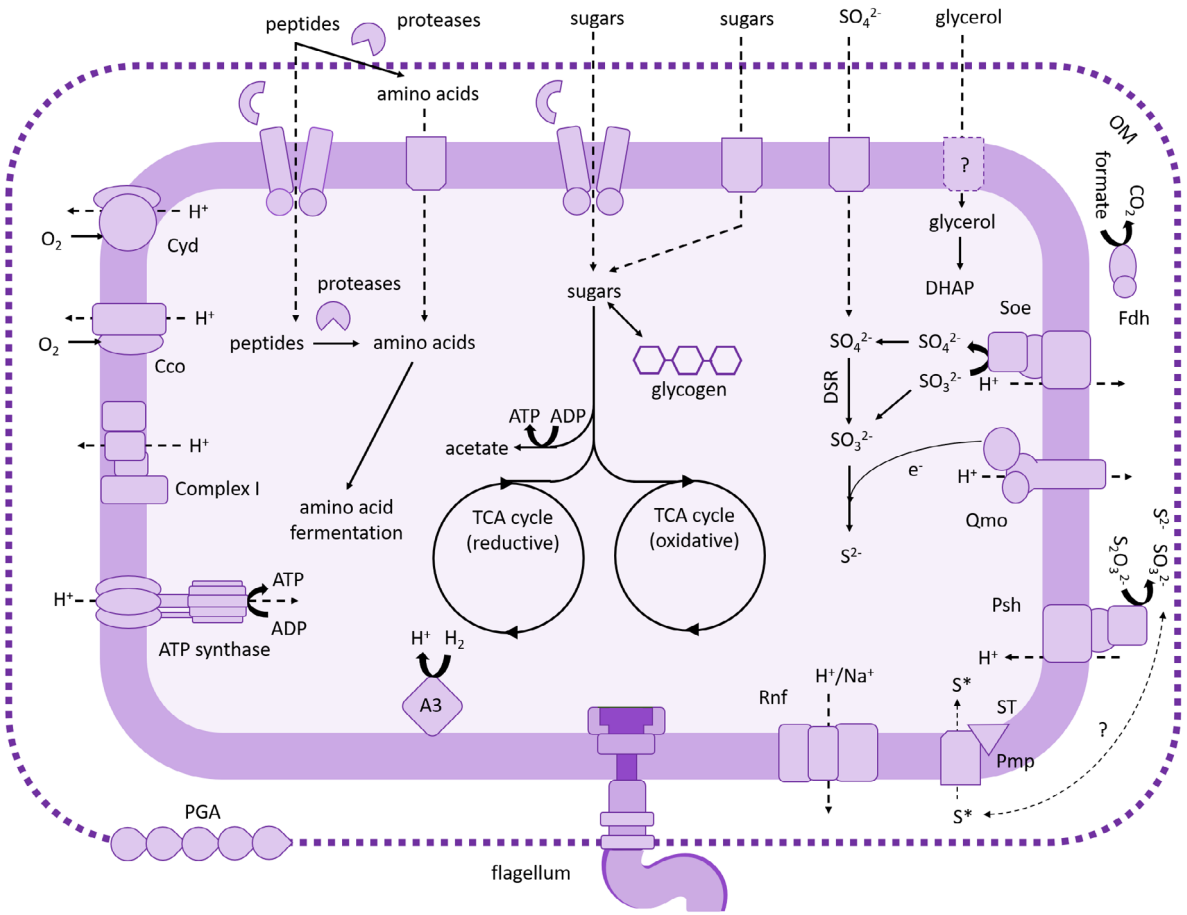

Fig. 4. Metabolic capacities of *Candidatus* Electryonea clarkiae (candidate phylum Electryoneota) as inferred from MAG sequences. The transporter by which glycerol enters the cytoplasm is not known. The identity of the sulfur species transported by the sulfur compound transporter (Pmp) is not known, and the function of the sulfurtransferase (ST) is also not known; both are encoded in the same gene cluster as thiosulfate reductase (Phs). One possibility, presented here, is that an unknown sulfur species (S*) that is a product of thiosulfate reduction is taken up by Pmp. A3, [FeFe] hydrogenase Group A3; Cyd, cytochrome *bd* ubiquinol oxidase; Cco, *cbb3*-type cytochrome c oxidase; DHAP, dihydroxyacetone phosphate; DSR, dissimilatory sulfate reduction; Fdh, formate dehydrogenase; OM, outer membrane; PGA, poly- γ-glutamate; Qmo, quinone-modifying oxidoreductase complex; Rnf, ion-translocating ferredoxin:NAD^+ oxidoreductase complex; Soe, sulfite dehydrogenase.

or hydrogen as substrates (Kublanov *et al*., 2017) (see Supplementary Information: Other sulfur metabolism enzymes). A function of Phs in *C*. *abyssi* fermentation is consistent with the proposed function of Phs in *S*. *enterica*, in which thiosulfate reduction is mainly an adjunct to a fermentative metabolism, rather than used for respiration (Heinzinger *et al*., 1995; Hinsley and Berks, 2002; Stoffels *et al*., 2012). Thus, we propose that *Ca*. Electryonea clarkiae has a Phs that uses thiosulfate as an electron acceptor during fermentation, with thiosulfate reduction taking place in the periplasm. Immediately downstream of the three Phs genes (*phsABC*) in *Ca*. Electryonea clarkiae are two genes for sulfur compound transporters (PmpA/B) (Gristwood *et al*., 2011) and a sulfurtransferase gene (Table S1). A homologous gene cluster is encoded in *C*. *abyssi* (GenBank accession CP018099.1). These PmpA/B transporters contain a single sulfur compound transport domain, and are homologous to YeeE thiosulfate transporters, which contains two such domains (Tanaka *et al*., 2020). The identity of the sulfur species transported by PmpA/B and the function of the sulfurtransferase are unclear; but the gene cluster suggests that thiosulfate reduction catalysed by the *Ca*. Electryonea clarkiae Phs complex may have a metabolic function outside of fermentation.

The heterotrophic abilities of Ace Lake *Ca*. Electryoneota appear to be directed toward the breakdown of proteinaceous matter, with amino acids utilized by further

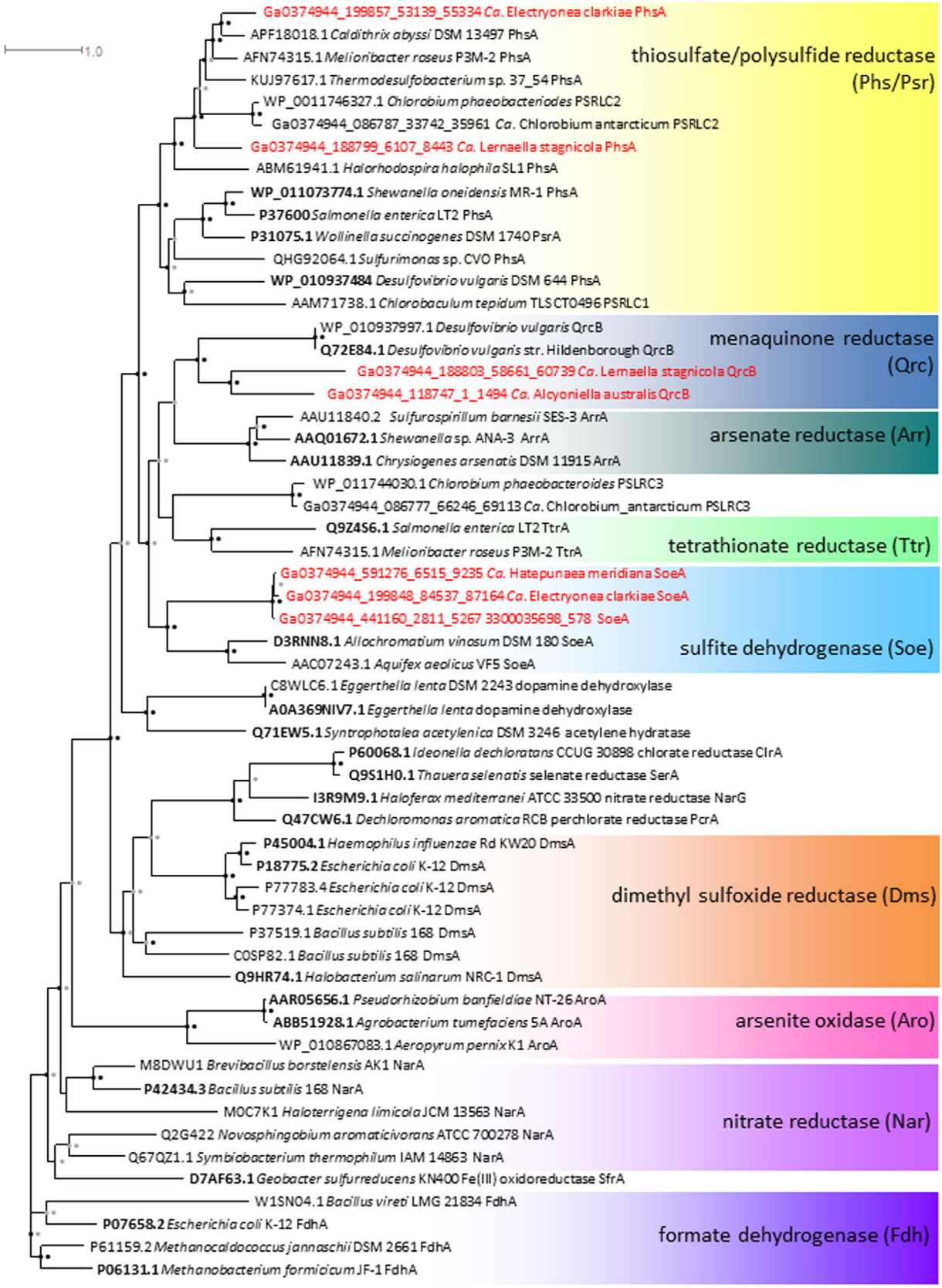

Fig. 5. Legend on next page.

catabolism. In MAGs of both *Ca*. Electryonea clarkiae and *Ca*. Hatepunaea meridiana very few genes for poly- or oligosaccharide degradation enzymes were detected, in contrast to numerous genes for proteases and peptidases, many of which are predicted to be serine proteases of the subtilisin family (Peptidase S8) (Table S1). Most of the latter have N-terminal signal peptides, which suggest an extracytoplasmic location. *Ca*. Electryonea clarkiae possesses genes for the degradation of amino acids including the catabolism of *trans*-4-hydroxy-L-proline to glutamate (Levin *et al*., 2017). *Ca*. Electryonea clarkiae MAGs encode VOR and IOR genes for BCAA and aromatic amino acid fermentation respectively (Schut *et al*., 2001; Daebeler *et al*., 2018); in addition to VOR and IOR, a branched-chain α-keto acid dehydrogenase complex is also encoded in *Ca*. Electryonea clarkiae, which like VOR uses branched-chain oxoacids as substrates (Venugopal *et al*., 2011).

The MAGs of both *Ca*. Electryonea clarkiae and *Ca*. Hatepunaea meridiana each encode a protein that is homologous to both trimethylamine:corrinoid methyltransferase (MttB) and glycine betaine:corrinoid methyltransferase (MtgB) (Ticak *et al*., 2014). In general across bacteria and archaea, MttB includes a genetically encoded pyrrolysine residue, which is not present in MtgB. There is no evidence for pyrrolysine in the sequences of the *Ca*. Electryoneota MttB/MtgB homologues. Phylogenetic analysis recovered the *Ca*. Electryoneota proteins as belonging to a larger clade of uncharacterized proteins separate from both MtgB and MttB, but more closely related to MttB (Fig. S2). In MAGs of both *Ca*. Electryonea clarkiae and *Ca*. Hatepunaea meridiana, each MttB/MtgB homologue is encoded in the same gene cluster as three genes that encode homologues of three of the four modules of cobalamin-dependent methionine synthase (MetH) (Evans *et al*., 2004): homocysteine-binding domain, cobalamin-binding domain (=corrinoid protein), and S-adenosylmethionine-binding activation domain (Fig. S3). This gene cluster (non-pyrrolysine MtgB/MttB homologue, homocysteine S-methyltransferase, corrinoid protein, activation protein) is found in diverse bacteria (Table S4), and we hypothesize that this MttB/MtgB homologue catalyses a novel corrinoid-dependent mechanism of methyl transfer for methionine synthesis, using an unknown methyl donor. A more typical multi-domain cobalamin- and THF-dependent methionine synthase (Evans *et al*., 2004) is also encoded in MAGs of both *Ca*. Electryonea clarkiae (1115 amino acids) and *Ca*. Hatepunaea meridiana (1223 amino acids), suggesting versatility in one-carbon metabolism.

Ace Lake *Ca*. Electryoneota MAGs also encode possible autotrophic abilities. The *Ca*. Electryonea clarkiae MAG encodes a citrate synthase that, among experimentally characterized citrate synthases, shows the highest sequence identity (47%) to the reversible citrate synthase of *Thermosulfidibacter takaii*, which employs this citrate synthase as part of a reverse TCA cycle (Nunoura *et al*., 2018). In addition, *Ca*. Electryonea clarkiae encodes a cytoplasmic, bifurcating [FeFe] hydrogenase (Group A3), and fumarate reductase. We propose that *Ca*. Electryonea clarkiae has the potential for chemolithoautotrophy that involves carbon fixation via a reverse TCA cycle driven by hydrogen oxidation catalysed by a bifurcating hydrogenase, as described for *T. takaii* (Nunoura *et al*., 2018). The same proteins as *Ca*. Electryonea clarkiae are encoded in the *Ca*. Hatepunaea meridiana MAG (including citrate synthase 49% match to *T. takaii* citrate synthase), with the exception of a hydrogenase gene, which is lacking in the *Ca*. Hatepunaea meridiana MAG.

The *Ca*. Electryonea clarkiae MAGs possess a complete set of genes for flagellar motility, whereas the *Ca*. Hatepunaea meridiana MAG encodes a complete set except for flagellin genes. Flagellin genes were reported previously in members of this phylum (Youssef *et al*., 2019a). MAGs of both *Ca*. Electryonea clarkiae and *Ca*. Hatepunaea meridiana encode poly-γ-glutamate synthetase (CapBC) and other proteins required for synthesis and transport of poly-γ-glutamate, a biopolymer involved in capsule formation, or released extracellularly as a water-binding component of a biofilm matrix (Rehm, 2010).

Fig. 5. Unrooted maximum-likelihood tree of Complex Iron–Sulfur Molybdoenzyme catalytic subunit homologues from select Ace Lake MAGs and reference sequences. Ace Lake sequences: IMG gene ID, taxonomy, red font. Reference sequences (accession ID, taxonomy, function; experimental evidence shown in bold font): P06131.1 (Shuber *et al*., 1986), P07658.2 (Axley *et al*., 1990), D7AF63.1 (Kaufmann and Lovley, 2001; Coppi *et al*., 2007), P42434.3 (Ogawa *et al*., 1995), ABB51928.1 (Kashyap *et al*., 2006), AAR05656.1 (Santini and vanden Hoven, 2004), Q9HR74.1 (Muller and DasSarma, 2005), P18775.2 (Weiner *et al*., 1988), P45004.1 (Loosmore *et al*., 1996), Q47CW6.1 (Bender *et al*., 2005), I3R9M9.1 (Lledo *et al*., 2004), Q9S1H0.1 (Schröder *et al*., 1997), P60068.1 (Thorell *et al*., 2003), Q71EW5.1 (Rosner and Schink, 1995), A0A369NIV7.1 (Maini Rekdal *et al*., 2019), D3RNN8.1 (Dahl *et al*., 2013), Q9Z4S6.1 (Winter *et al*., 2010), AAU11839.1 (Malasarn *et al*., 2004), AAQ01672.1 (Saltikov and Newman, 2003), Q72E84.1 (Venceslau *et al*., 2010), WP_010937484 (Aketagawa *et al*., 1985), P31075.1 (Krafft *et al*., 1992), P37600 (Clark and Barrett, 1987), WP_011073774.1 (Burns and DiChristina, 2009). PSRLC, polysulfide reductase-like complex; this notation for uncharacterized CISM superfamily proteins from green sulfur bacteria (Chlorobi) follows Frigaard and Bryant (2008). PSLRC3 is inferred to be sulfite oxidase (Frigaard and Bryant, 2008; Gregersen *et al*., 2011). Dots located on and to the right of nodes indicate the SH-aLRT branching support and ultrafast bootstrap support respectively. Black dot = 90%–100% support; grey dot = 50%–89% support; no dot indicates <50% support.

Phylum Candidatus Lernaellota (=FEN-1099)

Two Ace Lake MAGs (both 98% complete) represent candidate phylum FEN-1099, which is here named phylum *Candidatus* Lernaellota phylum nov. Each MAG represents a separate genus and species: *Ca*. Lernaella stagnicola gen. et sp. nov. [3300035698_1648 (type)]; *Ca*. Alcyoniella australis gen. et sp. nov. [3300035698_1390 (type)] (Table 4). The *Ca*. Lernaella stagnicola MAG encodes a cytochrome *bd* ubiquinol oxidase for aerobic respiration under low-O_2 conditions (Fig. 6); no aerobic respiration genes were found in the *Ca*. Alcyoniella australis MAG. *Ca*. Alcyoniella australis encodes citrate *(Re)*-synthase, which [unlike citrate *(Si)*-synthase, encoded in *Ca*. Lernaella stagnicola] is oxygen-sensitive and only found in strict anaerobes (Li *et al*., 2007; Marco-Urrea *et al*., 2011). *Ca*. Lernaella stagnicola and *Ca*. Alcyoniella australis MAGs were most abundant in the anoxic zone (1.5% and 0.64% respectively), although the former had much higher relative abundance in the oxic–anoxic interface than the latter did (Table S3).

The *Ca*. Lernaella stagnicola MAG encodes glycerol kinase and an anaerobic glycerol-3-phosphate dehydrogenase (GlpABC) (Varga and Weiner, 1995), suggesting that oxidation of glycerol-3-phosphate could be used to directly reduce the menaquinone pool. Both *Ca*. Lernaella stagnicola and *Ca*. Alcyoniella australis MAGs encode a four-subunit complex that we interpret as menaquinone reductase (Qrc) (Fig. 5). In the *Ca*. Lernaella stagnicola MAG, the entire membrane-bound complex is encoded (QrcABCD), comprising the multiheme cytochrome *c* protein (QrcA) and three CISM complex subunits (the gene cluster is incomplete in the *Ca*. Alcyoniella australis MAG). The membrane-bound Qrc of *Desulfovibrio vulgaris* catalyses the reduction of the menaquinone pool using electrons derived from the oxidation of H_2 or formate, with the QrcD subunit proposed to be capable of proton translocation (Venceslau *et al*., 2010). MAGs of *Ca*. Lernaella stagnicola and *Ca*. Alcyoniella australis both encode a periplasmic formate dehydrogenase (FdhAB) that lacks a membrane subunit for direct reduction of the menaquinone pool, as also found in *D. vulgaris* (da Silva *et al*., 2013); thus, as in the latter (Venceslau *et al*., 2010), the Qrc in *Ca*. Lernaellota species likely also uses formate as an electron donor. Unlike what was proposed for *D. vulgaris* (Venceslau *et al*., 2010), there is no evidence that the Qrc complex is linked to DSR in these *Ca*. Lernaellota MAGs; for the latter, the reduced menaquinone pool could possibly be re-oxidized using a cytoplasmic hydrogenase or fumarate reductase, although the precise mechanism(s) could not be deduced.

The *Ca*. Lernaella stagnicola MAG encodes a second CISM that is a possible Phs and includes a periplasmic PhsA subunit (Fig. 5). Immediately downstream of the genes for PhsABC are PmpA/B sulfur compound transporter and sulfurtransferase genes (Table S1), similar to what we found in *Ca*. Electryonea clarkiae MAGs (see *Phylum Candidatus Electryoneota* (=*AABM5-125-24*), above), except that one of the two PmpA/B transporters in *Ca*. Lernaella stagnicola MAG also contains a sulfurtransferase domain. As proposed for *Ca*. Electryonea clarkiae, this *Ca*. Lernaella stagnicola Phs-containing gene cluster may encode proteins involved in uptake and/or conversion of other sulfur compounds in addition to thiosulfate.

The *Ca*. Lernaella stagnicola MAG encodes three hydrogenases, all inferred to be cytoplasmic. Two are reversible: an [NiFe] NADH-dependent hydrogenase (Group 3d) and a bifurcating [FeFe] hydrogenase (Group A3) (Søndergaard *et al*., 2016). Additionally, a [FeFe] hydrogenase (Group C3) is encoded by a gene adjacent to the Group A3 hydrogenase gene; Group C3 hydrogenases have been postulated to have an H_2-sensory role (Søndergaard *et al*., 2016), consistent with the presence of a histidine kinase domain in the *Ca*. Lernaella stagnicola Group C3 hydrogenase. *Ca*. Alcyoniella australis encodes a single [NiFe] hydrogenase (Group 3d); in this case, the hydrogenase may function to oxidize H_2 to generate reductant for CO_2 fixation (Søndergaard *et al*., 2016), given that *Ca*. Alcyoniella australis encodes an almost complete Wood–Ljungdahl pathway, with the carbonyl branch (CODH-ACS) and most of the methyl branch (all enzymes except Fhs) present in the MAG. Thus, CO_2 may be successively fixed by CODH-ACS and POR to generate acetyl-CoA and pyruvate, respectively (Ragsdale and Pierce, 2008).

Based on the many GHs and proteases/peptidases encoded in the two MAGs, both *Ca*. Lernaella stagnicola and *Ca*. Alcyoniella australis are predicted to be proficient at saccharolysis and proteolysis. Abundant sulfatase genes in the *Ca*. Lernaella stagnicola MAG may serve to release sulfate from sulfated polysaccharides to make the latter more amenable to degradation [see Phylum Candidatus Hinthialibacterota (=*OLB16*), above]. *Ca*. Lernaella stagnicola and *Ca*. Alcyoniella australis MAGs possess genes for rhamnose and xylose degradation; no BMC genes were found, but the MAGs encode multiple aldehyde:ferredoxin oxidoreductases for detoxification of lactaldehyde, a byproduct of rhamnose degradation. Both *Ca*. Lernaella stagnicola and *Ca*. Alcyoniella australis encode complete glycolysis and gluconeogenesis pathways, and a complete oxidative TCA cycle. *Ca*. Lernaella stagnicola additionally encodes both enzymes of the glyoxylate bypass (isocitrate lyase, malate synthase), allowing acetate and glyoxylate to be used as carbon sources. *Ca*. Lernaella stagnicola and *Ca*. Alcyoniella australis MAGs also encode enzymes for fermentation of certain amino acids: BCAA, aromatic amino

Table 4. Summary of the physiological and metabolic traits inferred from two Ace Lake MAGs of phylum *Candidatus* Lernaellota phylum nov.

***Candidatus* Lernaella stagnicola** gen. et sp. nov.
Genus named after Lerna, a mythical lake and portal to the underworld; species name means 'stagnant lake dweller'
3300035698_1648 (type): 98% complete, 0.9% contamination
Highest abundance: 1.5% (19 m, anoxic zone)
Glycolysis, gluconeogenesis (includes both ATP-dependent and PP_i-dependent 6-phosphofructokinase)
TCA cycle (oxidative) [includes citrate *(Si)*-synthase]
Glyoxylate bypass
Pentose phosphate pathway (non-oxidative)
Aerobic respiration: cytochrome *bd* respiratory O_2 reductase, high O_2 affinity
NADH-quinone oxidoreductase (complex I)
F-type ATP synthase
Ion-translocating ferredoxin:NAD+ oxidoreductase Rnf complex
Na^+-translocating NADH-quinone reductase Nqr complex
Anaerobic glycerol-3-phosphate oxidation
Formate oxidation linked to menaquinone reductase complex
Thiosulfate reduction
Cytoplasmic [NiFe] hydrogenase, NAD-coupled (Group 3d); cytoplasmic [FeFe] hydrogenase, bifurcating (NAD, ferredoxin) (Group A3): used for H_2 oxidation and/or fermentation
Cytoplasmic [FeFe] hydrogenase (Group C3): sensory?
Assimilatory sulfate reduction
Glycoside hydrolases: 27 (14 with signal peptide)
Glycogen synthesis
Sulfatases: 14 (11 with signal peptide)
Proteases/peptidases: 33 (18 with signal peptide)
Degradation of rhamnose, xylose, aldehydes, aspartate, methionine, histidine, tyrosine, tryptophan, glycerol, formate, lactate, alcohols, aldehydes, sarcosine, phosphoglycolate
Fermentation of aromatic amino acids, glutamate, lysine
Synthesis of almost all 20 amino acids required for protein synthesis
Poly-γ-glutamate synthesis
Polyhydroxyalkanoate synthesis
ABC transporters: sugars, peptides, cobalamin, riboflavin, phosphate, Zn
Other transporters: sugars, peptides, amino acids, carboxylates, formate, lactate, nucleobases, phosphate, sulfate, Fe(II), Zn, Mg
Catalase, desulfoferrodoxin, hydroxylamine reductase
Flagella
***Candidatus* Alcyoniella australis** gen. et sp. nov.
Genus named after Alcyonia, a mythical lake and portal to the underworld; species name means 'southern'
3300035698_1390 (type): 98% complete, 1.9% contamination
Highest abundance: 0.64% (19 m, anoxic zone)
Glycolysis, gluconeogenesis (includes both ATP-dependent and PP_i-dependent 6-phosphofructokinase)
TCA cycle (oxidative) [includes citrate *(Re)*-synthase]
Pentose phosphate pathway (non-oxidative)
NADH-quinone oxidoreductase (complex I)
F-type ATP synthase
Ion-translocating ferredoxin:NAD+ oxidoreductase Rnf complex
Na^+-translocating NADH-quinone reductase Nqr complex
Cytoplasmic [NiFe] hydrogenase, NAD-coupled (Group 3d): used for H_2 oxidation and/or fermentation
Formate oxidation linked to menaquinone reductase complex
Wood–Ljungdahl pathway
Glycoside hydrolases: 25 (12 with signal peptide)
Trehalose and glycogen synthesis
Proteases/peptidases: 25 (15 with signal peptide)
Degradation of rhamnose, xylose, aspartate, histidine, tryptophan, glycerol, alcohols, aldehydes, sarcosine, phosphoglycolate
Fermentation of BCAA, aromatic amino acids, glutamate
Synthesis of almost all 20 amino acids required for protein synthesis
Polyhydroxyalkanoate synthesis
ABC transporters: sugars, peptides, cobalamin, Zn, Mn, Co/Ni, tungstate
Other transporters: sugars, peptides, carboxylates, nucleobases, phosphate, Fe(II), Zn, Mg, Co
Catalase, desulfoferrodoxin, hydroxylamine reductase

The complete etymologies of genera and species are given in Table S2.

acids, lysine, glutamate (Barker *et al*., 1982; Buckel, 2001; Daebeler *et al*., 2018). In addition, both MAGs are notable for encoding enzymes for the deamination of various amino acids (e.g. aspartate, methionine, histidine, tyrosine, tryptophan), potentially allowing their utilization as ammonia sources.

Ecosystem contributions of the new Ace Lake candidate phyla

Interrogation of the 12 Ace Lake MAGs enabled new metabolic traits to be inferred for four candidate phyla of Bacteria: Auribacterota (SURF-CP-2), Hinthialibacterota

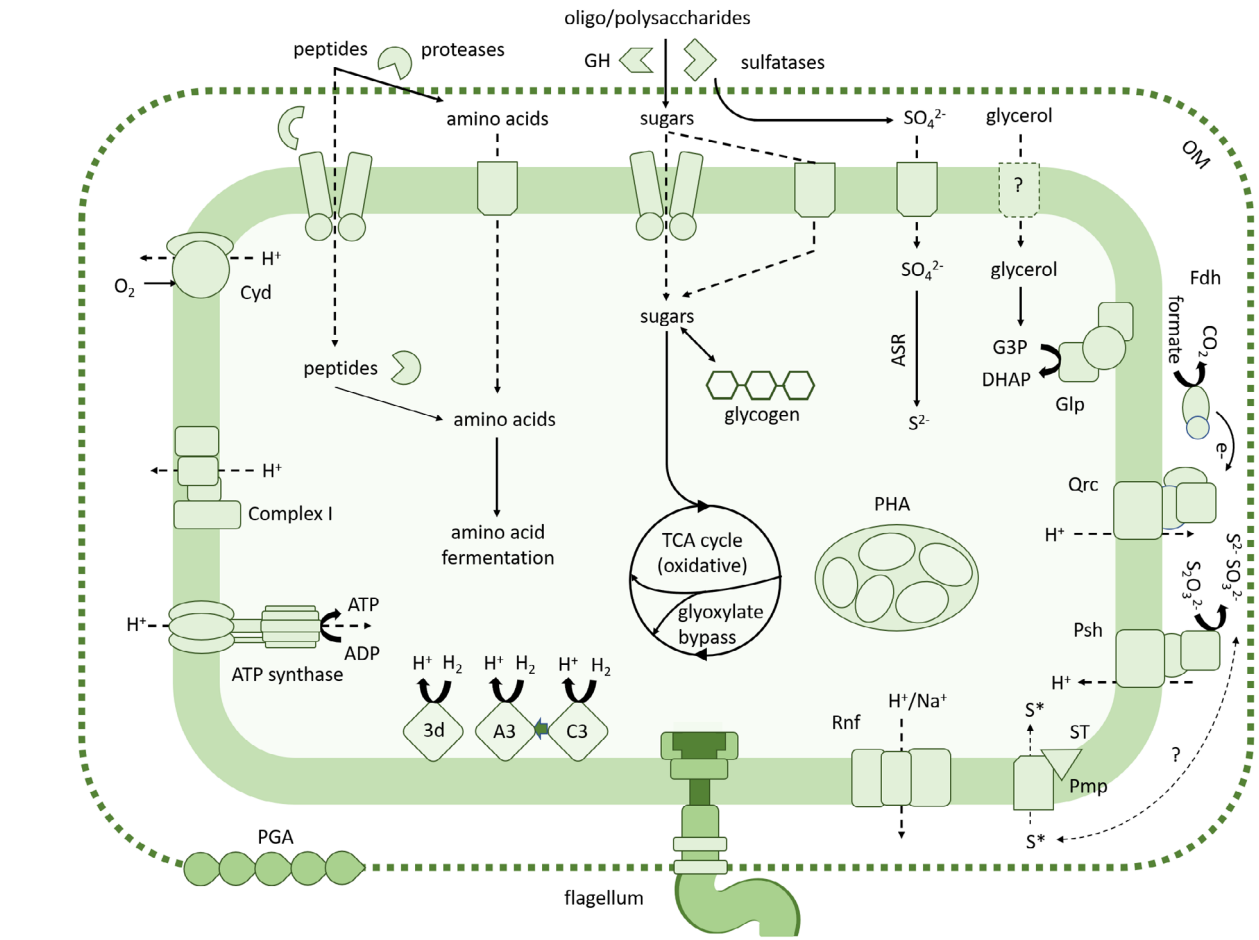

Fig. 6. Metabolic capacities of *Candidatus* Lernaella stagnicola (candidate phylum Lernaellota) as inferred from MAG sequences. Oligo/polysaccharides include both sulfated and non-sulfated oligo/polysaccharides. The transporter by which glycerol enters the cytoplasm is not known. For the possible functions of the sulfur compound transporter (Pmp) and sulfurtransferase (ST), see Fig. 4. 3d, [NiFe] hydrogenase Group 3d; A3, [FeFe] hydrogenase Group A3; ASR, assimilatory sulfate reduction; C3, [FeFe] hydrogenase Group C3 (sensory); Cyd, cytochrome *bd* ubiquinol oxidase; DHAP, dihydroxyacetone phosphate; Fdh, formate dehydrogenase; G3P, glycerol-3-phosphate; GH, glycoside hydrolases; Glp, anaerobic glycerol-3-phosphate dehydrogenase; OM, outer membrane; PHA, polyhydroxyalkanoate; Phs, thiosulfate reductase; Qrc, menaquinone reductase; Qmo, quinone-modifying oxidoreductase complex; PGA, poly-γ-glutamate; Rnf, ion-translocating ferredoxin:NAD^+ oxidoreductase complex; S*, unknown sulfur species; TCA, tricarboxylic acid.

(OLB16), Electryoneota (AABM-125-24), and Lernaellota (FEN-1099). By considering the metabolic potential of the new candidate phyla in combination with relative abundance calculations by depth, understanding of the physicochemical characteristics of the zones they inhabit, and knowledge of other lake taxa, we were able to infer broader ecosystem contributions. MAGs of *Ca*. Hinthialibacterota and *Ca*. Lernaellota encode numerous enzymes used for the degradation of polysaccharides (including fucoidan, in the case of the former), and MAGs of *Ca*. Electryoneota and *Ca*. Lernaellota encode numerous enzymes required for the degradation of polypeptides. This suggests that these three phyla contribute to the degradation of polymeric organic matter in Ace Lake, especially below the oxic zone. Thus, these new phyla add to the repertoire of Ace Lake bacteria inferred to degrade recalcitrant organic material and particulate matter, including Bacteroidota, Verrucomicrobiota, Planctomycetota, Gammaproteobacteria, and *Ca*. Cloacimonadota (Panwar *et al*., 2020; Williams *et al*., 2021a). We inferred the presence of a Wood–Ljungdahl pathway in certain MAGs belonging to *Ca*. Auribacterota and *Ca*. Lernaellota; however, in the absence of genes required for TCA cycle reversal (Schuchmann and Müller, 2016; Youssef *et al*., 2019b), the Wood–Ljungdahl pathway cannot support autotrophic growth in these taxa. Only in *Ca*. Electryonea clarkiae (*Ca*. Electryoneota) could we reconstruct a complete

autotrophic pathway, in this case by using the reverse TCA cycle.

Members of all four new phyla are inferred to contribute to sulfur cycling in Ace Lake, including by the cycling of inorganic sulfur species and mineralization of sulfated organic compounds (Fig. 7). During the summer months, the oxic–anoxic interface of Ace Lake is dominated by *Ca*. Chlorobium antarcticum and sulfate-reducing Desulfobacterota, which together constitute the centrepiece of a sulfur cycle in which *Ca*. Chlorobium antarcticum uses sulfide as an electron donor, oxidizing it to sulfate that is used by Desulfobacterota for DSR, which generates sulfide (Ng *et al*., 2010; Lauro *et al*., 2011; Panwar *et al*., 2020) (Fig. 7; Fig. S1). We interpret *Ca*. Electryoneota in Ace Lake as being capable of DSR, and therefore may also be metabolically linked to *Ca*. Chlorobium antarcticum. We posit that sulfur and thiosulfate reducers of the phyla *Ca*. Auribacterota and *Ca*. Lernaellota also benefit from sulfur species generated as intermediates in the complete oxidation of sulfide to sulfate by *Ca*. Chlorobium antarcticum. These taxa would therefore provide a source of sulfide to Ace Lake that augments the contribution made by dissimilatory sulfate reducers.

All five Ace Lake *Ca*. Auribacterota species encode a complete sulfhydrogenase, which to the best of our knowledge has not been previously reported for this phylum. *Ca*. Chlorobium antarcticum would be a major source of elemental (zero-valence) sulfur in Ace Lake. In general, GSB oxidize sulfide to sulfur globules, which are stored and degraded extracellularly (including at a distance from the cell) before being further oxidized to sulfate; it has been proposed that the extracellular location of elemental sulfur benefits GSB by providing extracellular sulfur to sulfur-reducing bacteria, thereby facilitating the generation of sulfide (Marnocha *et al*., 2016). Not all sulfur needs to be converted to sulfate for GSB growth to occur (Holkenbrink *et al*., 2011), and the retention of sulfur globules may be advantageous under dark conditions because sulfur (but not sulfate) can be used by GSB as an electron acceptor during fermentation of storage carbohydrate (Brune, 1989; Holkenbrink *et al*., 2011); thus, sulfur reduction may allow survival of *Ca*. Chlorobium antarcticum in Ace Lake during the prolonged darkness

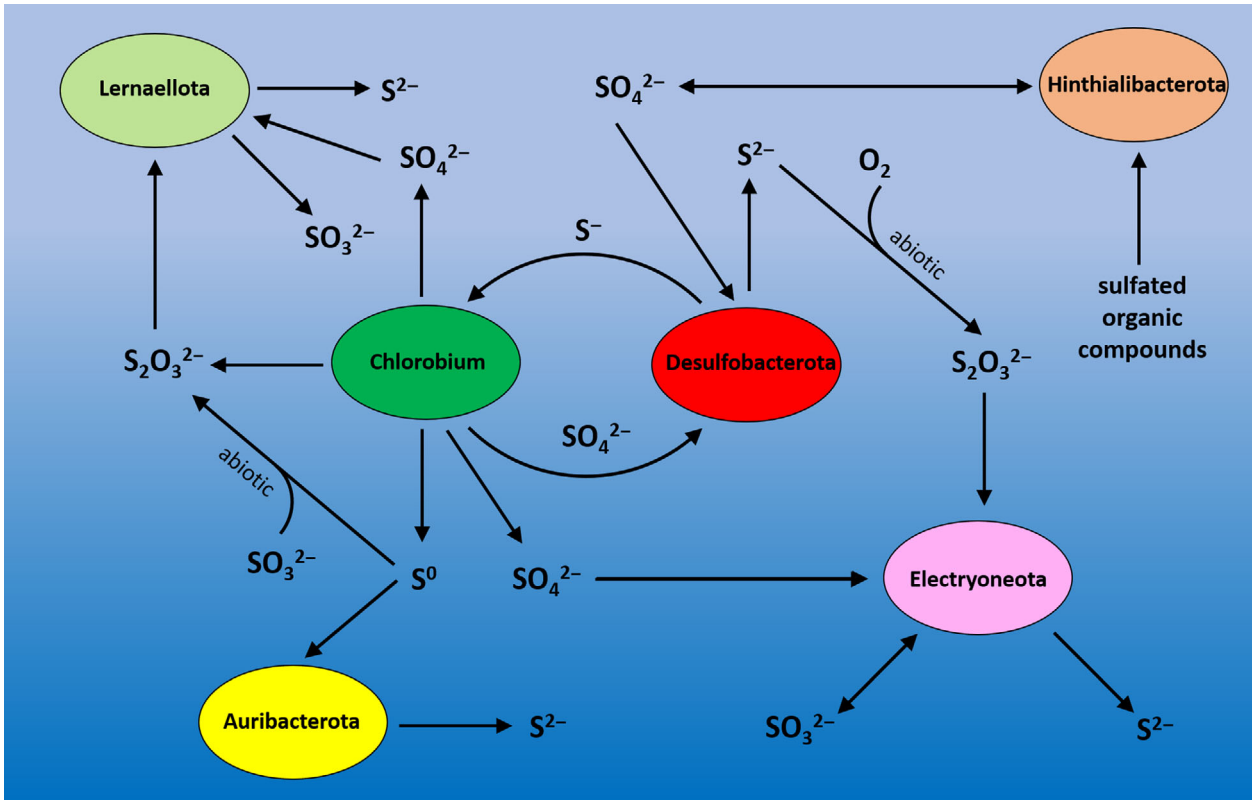

Fig. 7. Predicted roles in sulfur cycling played by members of four candidate phyla (Auribacterota, Hinthialibacterota, Electryoneota, Lernaellota) in the Ace Lake ecosystem. Only the predicted roles of the four aforementioned phyla and the dominant sulfur cycling taxa *Candidatus* Chlorobium antarcticum and Desulfobacterota are depicted here. The relative abundances of the six taxa are not equivalent. Double-headed arrows indicate that the sulfur compound is generated and assimilated by different processes by the same taxon.

of the polar winter. Biogenic elemental sulfur would therefore be readily available in Ace Lake for anaerobic sulfur reducers. The abundance of sulfhydrogenase, based on catalytic subunit ShyC (K17995), was found to be comparable across multiple depths in the interface and anoxic zone (Fig. 8; Fig. S4), which is consistent with the availability of elemental sulfur in these zones (Rankin *et al*., 1999). These sulfhydrogenases are encoded in representatives of diverse bacterial phyla in Ace Lake (Fig. 9A), including taxa previously implicated in sulfur reduction in Ace Lake (e.g. Desulfobacterota, *Ca*. Cloacimonadota, *Ca*. Omnitrophota) (Panwar *et al*., 2020; Williams *et al*., 2021a), and phyla previously unreported from Ace Lake, including *Ca*. Auribacterota, as well as other phyla for which sulfhydrogenases have been reported in other environments (e.g. Elusimicrobiota, *Ca*. Margulisbacteria) (Matheus Carnevali *et al*., 2019; Méheust *et al*., 2020).

Unlike sulfhydrogenase, the distribution of Phs/Psr (based on the catalytic subunit PhsA/PsrA; both classified under K08352) in the Ace Lake water column peaked in abundance at the oxic–anoxic interface, and declined with increasing depth in the anoxic zone (Fig. 8; Fig. S4). The prevalence of Phs/Psr at the interface is partly due to the presence of PSLRC2 in *Ca*. Chlorobium antarcticum, previously reported in *Chlorobium phaeobacteroides* and of unknown function (Frigaard and Bryant, 2008); our phylogenetic analysis recovered PSLRC2 in the Phs/Psr group (Fig. 3). However, this decline in abundance of Phs/Psr with increased depth in Ace Lake is apparent even after *Ca*. Chlorobium antarcticum is removed from the dataset (Fig. 8; Fig. S4). This distribution is consistent with Phs/Prs acting on thiosulfate. Thiosulfate forms abiotically in the environment by chemical reaction between dissolved sulfide and oxygen (Gregersen *et al*., 2011), the latter available only in oxygenated waters. Thiosulfate is also generated by GSB during sulfide oxidation to sulfate, possibly as an adventitious byproduct of the reaction of the transient intermediate sulfite with other sulfur species (Gregersen *et al*., 2011; Holkenbrink *et al*., 2011). Unlike many GSB, *Ca*. Chlorobium antarcticum lacks the Sox system for thiosulfate oxidation (Ng *et al*., 2010; Panwar *et al*., 2021). Thus, thiosulfate generated and exported by *Ca*. Chlorobium antarcticum could be utilized by other bacteria, including Gammaproteobacteria in the oxic zone that encode Sox systems (Panwar *et al*., 2021), and by diverse bacteria in the anoxic zone that encode Phs, including *Ca*. Electryonea clarkiae (*Ca*. Electryoneota) and *Ca*. Lernaella stagnicola (*Ca*. Lernaellota) (Fig. 9B). Moreover, reduction of thiosulfate generates both sulfide and sulfite as products, and it has been proposed that sulfite released from cells can react with elemental sulfur in the environment to generate further thiosulfate, thereby sustaining an intracellular sulfur cycle (Hinsley and Berks, 2002; Burns and DiChristina, 2009), as well as consuming elemental sulfur in the ecosystem. Sulfite could also be used as an energy source in *Ca*. Electryoneota using sulfite dehydrogenase. Furthermore, the fact that the Phs complex is encoded in the same gene cluster as PmpA/B transporters and sulfurtransferases in *Ca*. Electryonea clarkiae and *Ca*. Lernaella stagnicola suggests that thiosulfate (and/or the products of thiosulfate reduction) could be utilized for other purposes in these bacteria.

In addition to sulfate being produced by *Ca*. Chlorobium antarcticum and other sulfide-oxidizing bacteria, it can also be generated biogenically by the action of sulfatases, which release sulfate from a broad range of sulfated compounds (Berteau *et al*., 2006). Sulfatase genes were detected throughout the Ace Lake water column (Fig. 8; Fig. S4). Sulfated organic compounds may be degraded to provide sulfate under conditions of sulfur limitation, or 'pruned' of sulfate groups to facilitate access to the carbon skeleton for utilization as nutrient sources (Kertesz, 1999). The latter was previously inferred to be important for aerobic members of the phyla Verrucomicrobiota, Planctomycetota, and Bacteroidota (Panwar *et al*., 2020), which dominate the Ace Lake taxa that encode sulfatases (Fig. 9C). *Ca*. Hinthialibacter antarcticus encodes numerous GH and sulfatase genes, and we infer that it uses sulfated organic compounds as sources of both carbon and sulfur (Table 2), including polysaccharides and glycosaminoglycans from algae in Ace Lake and terrestrial fauna in the vicinity of the lake.

To the best of our knowledge, we have ascribed ecological functions to the new Ace Lake species that have not previously been reported for the four 'dark matter' phyla: degradation of complex organic matter (*Ca*. Hinthialibacter antarcticus, *Ca*. Electryonea clarkiae, *Ca*. Hatepunaea meridiana, *Ca*. Lernaella stagnicola, *Ca*. Alcyoniella australis); ammonification by DNRA (*Ca*. Hinthialibacter antarcticus); and chemolithoautotrophy (*Ca*. Electryonea clarkiae, *Ca*. Hatepunaea meridiana). We also implicate these phyla in processes associated with sulfur cycling (sulfur reduction, thiosulfate reduction, sulfate ester hydrolysis), in addition to DSR, which was previously deduced for *Ca*. Electryoneota from other environments (Youssef *et al*., 2019a; Youssef *et al*., 2019b). The presence of some of the new species in non-Antarctic environments was indicated by finding matches (88%–100% identity) to sequences in the IMG 16S rRNA gene public assembled metagenomes database; diverse environments were represented, including marine sediments, meromictic ponds, salt marshes, the deep subsurface, a solar saltern, and uranium-contaminated floodplain (Table S2). In such environments it is likely the *Ca*. Auribacterota species would be

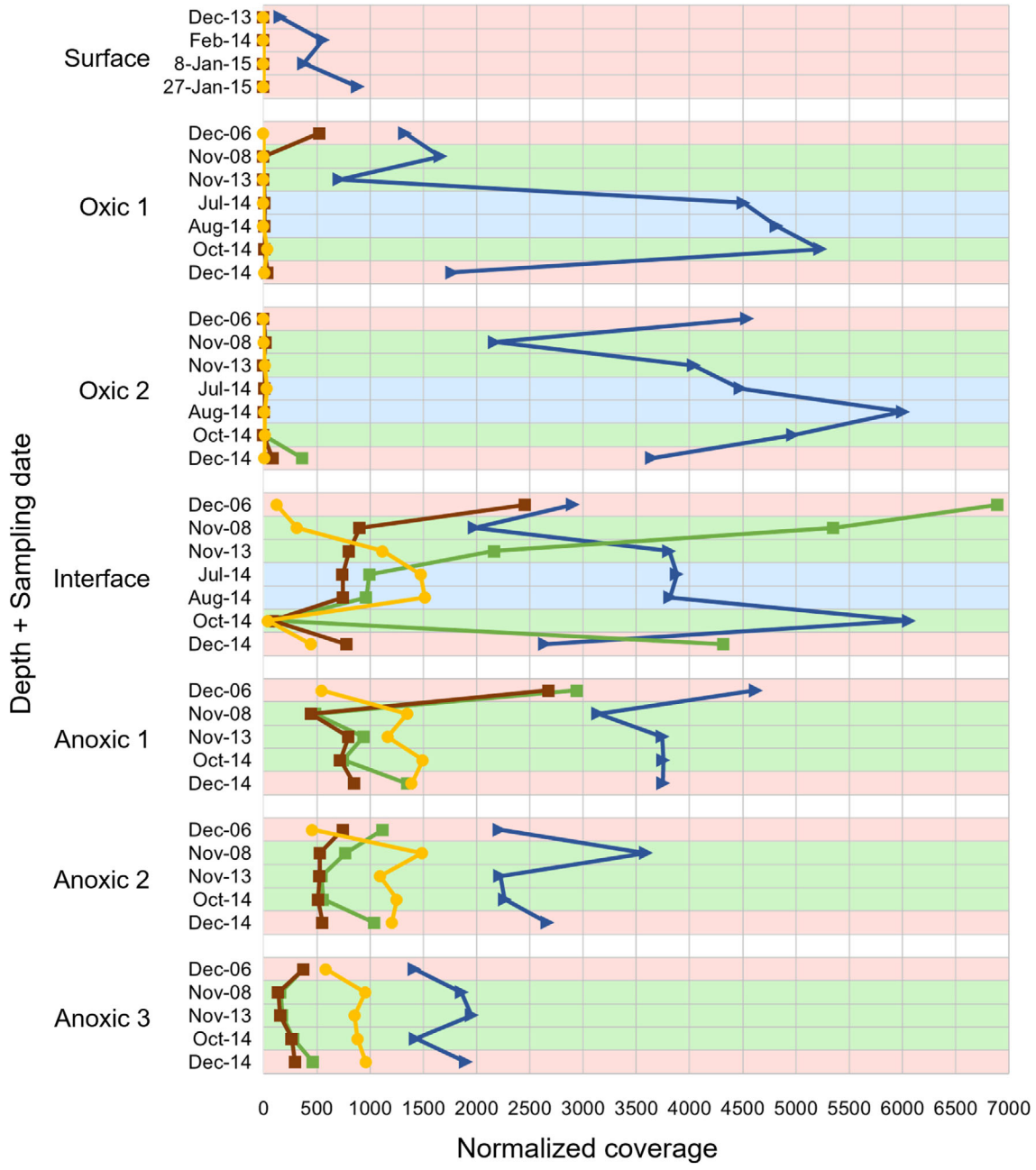

Fig. 8. Normalized coverage data for selected sulfur cycling enzymes across different depths and seasons in Ace Lake. Sulfhydrogenase, based on ShyC (K17995), the catalytic subunit of the sulfur reductase component of sulfhydrogenase (yellow circles); thiosulfate/polysulfide reductase, based on the catalytic subunit (PhsA/PsrA) (K08352), with the dataset including *Candidatus* Chlorobium antarcticum (green squares) or excluding *Ca*. Chlorobium antarcticum (brown squares); sulfatases (K01130; blue triangles). Metagenomes were from six lake depths: surface, 5 m (Oxic 1), 11.5–13 m (Oxic 2), 12.7–14.5 m (Interface), 14–16 m (Anoxic 1), 18–19 m (Anoxic 2) and 23–24 m (Anoxic 3). Seasons are highlighted by coloured background: red, summer (Dec, Jan, Feb); blue, winter (Jul, Aug); green, spring (Oct, Nov). Normalized coverages are for the metagenomes of the three size fractions (3.0, 0.8 and 0.1 μm) representing a single depth and sampling date (see Experimental procedures). For a logarithmic scale representation of this graph, refer to Fig. S4.

restricted to anoxic conditions, as it is in Ace Lake. By contrast, we interpret species of the phyla *Ca*. Hinthialibacterota, *Ca*. Electryoneota, and *Ca*. Lernaellota (with the exception of *Ca*. Alcyoniella australis) as facultative anaerobes, and certain species (*Ca*. Electryonea clarkiae, *Ca*. Hatepunaea meridiana, *Ca*. Lernaella stagnicola) capable of respiration under low-O_2 conditions, which may allow growth under a range of oxygen concentrations in aqueous environments. Knowledge of the metabolic potential of the four Ace Lake 'dark matter'

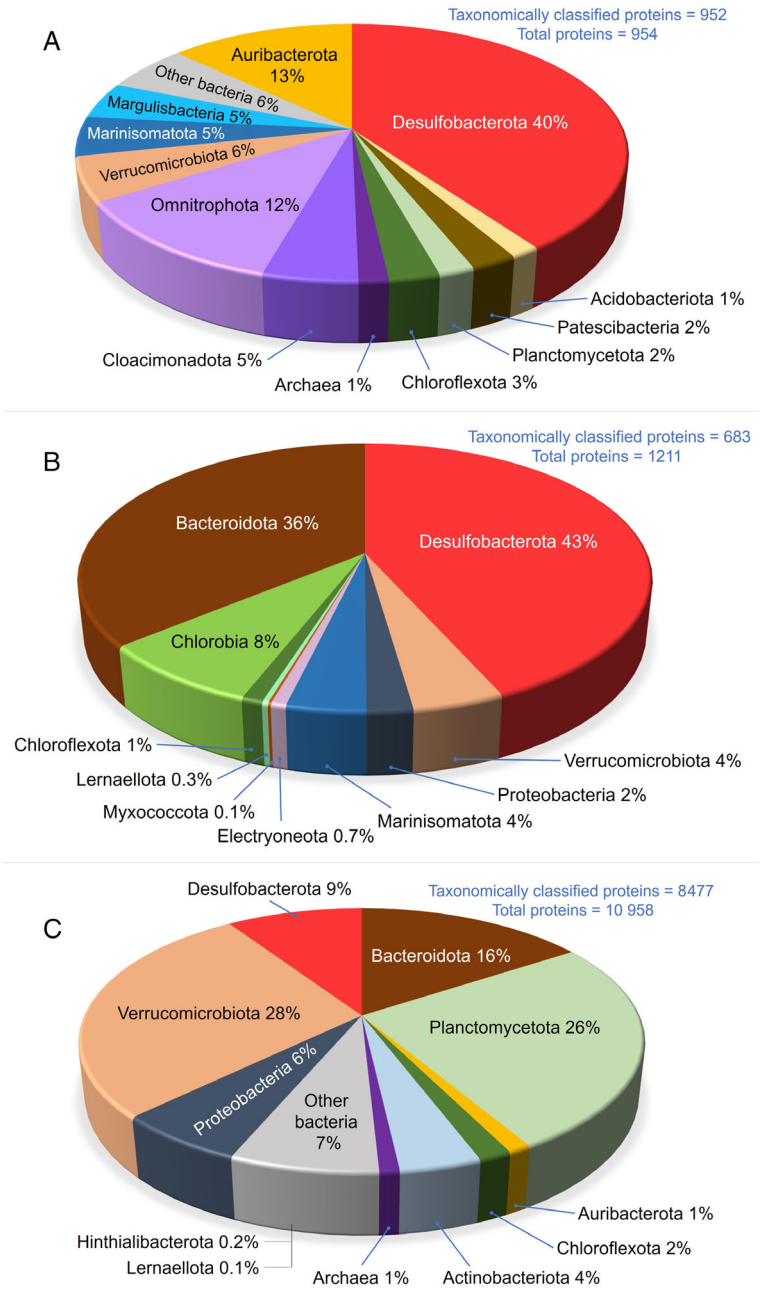

Fig. 9. Contribution of phylum-level taxa to functional potential in Ace Lake. Pie charts showing the percentage contribution for (A) sulfhydrogenase based on ShyC (K17995), (B) thiosulfate/polysulfide reductase based on PhsA/PsrA (K08352), (C) sulfatases (K01130). Thiosulfate/polysulfide reductase and sulfatase proteins were identified through KEGG analysis, as described previously (Panwar *et al*., 2020). Sulfhydrogenase (ShyC) proteins were identified through matches to reference ShyC protein sequences and KEGG analysis (see Experimental procedures). Proteins were taxonomically classified using GTDB taxonomy indicated in the Ace Lake co-assembly IMG data (IMG genome ID: 3300035698) (see Experimental procedures). Each taxon is consistently represented by a single colour in all plots. Note that, for convenience, class Chlorobia has been separated from phylum Bacteroidota in (B). Only taxonomically classified proteins are shown.

phyla combined with availability of their MAGs provides considerable scope for performing ecophysiological assessments of a range of environments for which metagenome data are becoming increasingly available (Nayfach *et al*., 2020).

Experimental procedures

Sample collection and sequencing

Microbial biomass was sampled from Ace Lake in the austral summers of 2006/2007 and 2008/2009, and a full Antarctic seasonal cycle of summer 2013/2014 to summer 2014/2015. Biomass was collected by sequential size fractionation through a 20 μm prefilter onto 3.0, 0.8- and 0.1-μm pore-sized, large format (293-mm polyethersulfone membrane) filters, and DNA was extracted from the biomass as described previously (Ng *et al*., 2010). Six depths were sampled: surface, 5, 11.5–13, 12.7–14.5 (oxic–anoxic interface), 14–16, 18–19 and 23–24 m with the precise depths varying depending on the water level in the lake (Panwar *et al*., 2020). In winter 2014, samples were not taken below the oxic–anoxic interface (Panwar *et al*., 2020). DNA sequences for 120 individual

metagenomes (Panwar *et al*., 2020) were uploaded to IMG (Huntemann *et al*., 2015). High- and medium-quality MAGs were auto-generated from individual metagenomes during the IMG pipeline process. QC_filtered raw reads from the individual Ace Lake metagenomes were co-assembled using Megahit v1.1.1 (Li *et al*., 2016) with a setting of meta-large, and MAGs were generated from the co-assembly using MetaBAT v2.12.1 with minContig length 2500 bp (Kang *et al*., 2019). MAGs from the co-assembly (available in IMG as Metagenome ID 3300035698) were assessed for completeness and contamination using CheckM v1.0.7 (Parks *et al*., 2015), for taxonomic identity using RefineM v 0.0.23 (Parks *et al*., 2017), and for phylogenetic placement using GTDB Toolkit (GTDB-Tk) v.1.4.0 with GTDB release R95 (Chaumeil *et al*., 2019; Parks *et al*., 2020) and dependencies as described previously (Williams *et al*., 2021a).

Relationship to other taxa, and biogeographic distribution

Phylogenetic trees were constructed using the classify and *de novo* workflows in GTDB-Tk and visualized using Dendroscope v3.5.7 (Huson and Scornavacca, 2012). Relationships between Ace Lake 'dark matter' MAGs and their nearest relatives in the GTDB-Tk reference tree were investigated using CompareM v0.1.1 (https://github.com/dparks1134/CompareM) to calculate average AAI and fastANI v 1.32 (Jain *et al*., 2018) to calculate ANI. To better understand the uniqueness and biogeographic distribution of these taxa, 16S rRNA genes present in the Ace Lake MAGs were used to query the IMG 'All Isolates' dataset (includes all isolates, MAGs and SAGs), the IMG '16S rRNA public assembled metagenomes 2021-09-24' dataset and the NCBI nt database (accessed 17-12-2021). MAG 3300035698_578 did not contain a 16S rRNA gene so for this MAG the 23S rRNA gene was used to query the IMG 'All Isolates' dataset, the IMG '23S rRNA public assembled metagenomes 2021-10-05' dataset and NCBI nt.

Genome annotation

The genomic functional potential of the MAGs was assessed by considering cellular and metabolic traits based upon manual examination of proteins and pathways that was performed in a similar way to previous assessments of the validity of gene functional assignments (Allen *et al*., 2019; Panwar *et al*., 2020; Williams *et al*., 2021a, 2021b). Instead of querying individual genes or pathways as the basis for predicting metabolic reconstructions, we used automated annotations as a starting point for a more rigorous approach: individual proteins annotated by IMG were vetted manually, and metabolic reconstructions were inferred by organizing these proteins into known pathways. Individual metabolic pathways inferred for each MAG were then connected to provide a comprehensive assessment of the predicted metabolic capacities of these taxa. The manual vetting process for each protein was as follows. Protein sequences were submitted to ExPASy BLAST or NCBI BLASTP (both using the 'UniProtKB/Swiss-Prot only' option); proteins needed to show ≥30% sequence identity over the length of the protein and/or an expectation (*E*) value $<10^{-10}$ (Pearson, 2013) to an experimentally verified protein in the ExPASy BLAST database for the functional annotation to be considered valid. If this threshold was not reached, protein sequences were submitted to InterProScan (Blum *et al*., 2020) to identify functional domains and potential subcellular locations, and in certain cases phylogenetic analysis was performed to help resolve the function of a protein [e.g. CISM superfamily enzymes, corrinoid:methyltransferases]. GH families were identified using CAZy (Carbohydrate-Active enZymes) classification (Lombard *et al*., 2014). Protein sequences that were initially identified as hydrogenases based on catalytic domains were classified further using HydDB (Søndergaard *et al*., 2016). IMG annotations that could not be verified using the aforementioned process were excluded from this study. All protein annotations in this study are putative, and a full list of proteins identified in this study has been provided (Table S1). MAGs were named according to recommendations for describing novel *Candidatus* species (Konstantinidis *et al*., 2017; Chuvochina *et al*., 2019; Murray *et al*., 2020). All MAGs used in this study, including type MAGs, etymologies, and supporting metadata, are provided in Table S2.

Functional potential analysis and determination of contributing taxa

IMG-generated KEGG orthology data were used to assess the functional potential of thiosulfate/polysulfide reductases (K08352), sulfhydrogenases (K17665), and sulfatases (K01130) in Ace Lake, using a previously described method (Panwar *et al*., 2020). Additional sulfhydrogenase proteins were identified through alignment of the protein sequences from 120 Ace Lake metagenomes to reference protein sequences of ShyC, the catalytic subunit of sulfhydrogenase. The alignment was performed using the blastp module of DIAMOND v0.9.31 (Buchfink *et al*., 2014) with *E* value 10^{-5} and 35% minimum alignment identity, and only alignments covering ≥50% of reference sequence lengths were considered. To determine contributing taxa, the proteins identified as thiosulfate/polysulfide reductases, sulfhydrogenases, and sulfatases were aligned to reference proteins in Ace Lake co-assembly MetaBAT data (IMG

genome ID: 3300035698), and the MAG taxonomies were used to classify the query proteins. The alignment was performed using the blastp module of DIAMOND v0.9.31 with *e*-value 10^{-5}, 35% minimum alignment identity, 50% minimum query cover and 50% minimum subject cover. To show the distribution of contributing taxa, the taxonomically classified proteins were plotted as pie charts.

Where specific protein families of interest were identified (CISM catalytic subunits; corrinoid:methyltransferase), multiple sequence alignments were created with the proteins of interest and selected reference sequences from Swiss-Prot or NCBI nr, and trees constructed using MEGA (Kumar *et al*., 2018) or IQ-TREE. For phylogenetic analysis of CISM catalytic subunit homologues, multiple sequence alignment was created using Muscle (Edgar, 2004), manually curated, and submitted to IQ-TREE webserver (Nguyen *et al*., 2015) for maximum-likelihood model selection (Kalyaanamoorthy *et al*., 2017), tree reconstruction, and ultrafast bootstrapping (1000 replicates; Hoang *et al*., 2017). Maximum-likelihood tree of corrinoid:methyltransferases was prepared with MEGA X v10.1.7 using MUSCLE algorithm for protein alignment and 1000 bootstrap replications.

Calculation of taxon abundances

The abundances of candidate phyla Auribacterota, Hinthialibacterota, Electryoneota, and Lernaellota MAGs were calculated using the contigs in the Ace Lake co-assembly MetaBAT data, similar to a previously described approach used for calculating operational taxonomic unit abundances (Panwar *et al*., 2020; Panwar *et al*., 2021). Here, the read depths of co-assembly MAG contigs and unbinned contigs in 119 Ace Lake metagenomes and contig lengths were used to calculate contig-based abundances (Panwar *et al*., 2020). The Dec. 2014 3–20 μm filter metagenome from the oxic–anoxic interface of Ace Lake was not available when the Ace Lake co-assembly MetaBAT data were generated, so this metagenome was not included in MAG abundance analyses. MAG relative abundance was calculated by dividing the MAG abundance in a metagenome by the total metagenome abundance (Panwar *et al*., 2020). Highest relative abundance of each MAG refers to peak relative abundance in a single metagenome (Panwar *et al*., 2020). The total metagenome abundance refers to the sum of abundances (average read depth × length) of all MAG contigs and unbinned contigs in a metagenome (Panwar *et al*., 2020). To generate Ace Lake depth/season abundance profiles of MAGs, the relative abundances of MAGs were plotted as bar charts.

Acknowledgements

This work was supported by the Australian Research Council (DP150100244) and the Australian Antarctic Science Program (project 4031). Computational analyses at UNSW Sydney were performed on the computational cluster Katana, supported by the Faculty of Science. We thank the JGI for providing long-term support for the Antarctic metagenomics project; the expeditioners and Helicopter Resources crew at Davis Station during the 2006–2007, 2008–2009 and 2013–2015 expeditions for their assistance in collecting samples, and the Australian Antarctic Division for technical and logistical support during the expeditions. We acknowledge the considerable value that the reviewers brought to this study during the review process. Open access publishing facilitated by University of New South Wales, as part of the Wiley - University of New South Wales agreement via the Council of Australian University Librarians. [Correction added on 25 May 2022, after first online publication: CAUL funding statement has been added.]

Authors' Contributions

T. J. Williams conceived the study and performed the primary analyses and writing of the manuscript. M. A. Allen and P. Panwar performed computational analyses. All authors participated in the interpretation of the findings and contributed to the writing of the manuscript. All authors read and approved the final manuscript.

Availability of Data

All metagenomes and medium and high-quality MAGs used in this study are available in IMG: Metagenome ID 3300035698, 3300031227 and 3300025642.

References

Adam, P.S., Borrel, G., and Gribaldo, S. (2018) Evolutionary history of carbon monoxide dehydrogenase/acetyl-CoA synthase, one of the oldest enzymatic complexes. *Proc Natl Acad Sci U S A* **115**: E1166–E1173.

Aketagawa, J., Kobayashi, K., and Ishimoto, M. (1985) Purification and properties of thiosulfate reductase from *Desulfovibrio vulgaris*, Miyazaki F. *J Biochem* **97**: 1025–1032.

Ale, M.T., Mikkelsen, J.D., and Meyer, A.S. (2011) Important determinants for fucoidan bioactivity: a critical review of structure-function relations and extraction methods for fucose-containing sulfated polysaccharides from brown seaweeds. *Mar Drugs* **9**: 2106–2130.

Allen, M.A., Lauro, F.M., Williams, T.J., Burg, D., Siddiqui, K. S., DeFrancisci, D., *et al*. (2019) The genome sequence of the psychrophilic archaeon, *Methanococcoides burtonii*: the role of genome evolution in cold adaptation. *ISME J* **3**: 1012–1035.

Axley, M.J., Grahame, D.A., and Stadtman, T.C. (1990) *Escherichia coli* formate-hydrogen lyase. Purification and properties of the selenium-dependent formate dehydrogenase component. *J Biol Chem* **265**: 18213–18218.

Barker, H.A., Kahn, J.M., and Hedrick, L. (1982) Pathway of lysine degradation in *Fusobacterium nucleatum*. *J Bacteriol* **152**: 201–217.

Bender, K.S., Shang, C., Chakraborty, R., Belchik, S.M., Coates, J.D., and Achenbach, L.A. (2005) Identification, characterization, and classification of genes encoding perchlorate reductase. *J Bacteriol* **187**: 5090–5096.

Berteau, O., Guillot, A., Benjdia, A., and Rabot, S.A. (2006) New type of bacterial sulfatase reveals a novel maturation pathway in prokaryotes. *J Biol Chem* **281**: 22464–22470.

Blum, M., Chang, H.Y., Chuguransky, S., Grego, T., Kandasaamy, S., Mitchell, A., *et al*. (2020) The InterPro protein families and domains database: 20 years on. *Nucleic Acids Res* **49**: D344–D354.

Borisov, V.B., Gennis, R.B., Hemp, J., and Verkhovsky, M.I. (2011) The cytochrome *bd* respiratory oxygen reductases. *Biochim Biophys Acta* **1807**: 1398–1413.

Brune, D.C. (1989) Sulfur oxidation by phototrophic bacteria. *Biochim Biophys Acta* **975**: 189–221.

Buchfink, B., Xie, C., and Huson, D.H. (2014) Fast and sensitive protein alignment using DIAMOND. *Nat Methods* **12**: 59–60.

Buckel, W. (2001) Unusual enzymes involved in five pathways of glutamate fermentation. *Appl Microbiol Biotechnol* **57**: 263–273.

Bunesova, V., Lacroix, C., and Schwab, C. (2016) Fucosyllactose and L-fucose utilization of infant *Bifidobacterium longum* and *Bifidobacterium kashiwanohense*. *BMC Microbiol* **16**: 248.

Burns, J.L., and DiChristina, T.J. (2009) Anaerobic respiration of elemental sulfur and thiosulfate by *Shewanella oneidensis* MR-1 requires *psrA*, a homolog of the *phsA* gene of *Salmonella enterica* serovar *typhimurium* LT2. *Appl Environ Microbiol* **75**: 5209–5217.

Burton, H.R., and Barker, R.J. (1979) Sulfur chemistry and microbiological fractionation of sulfur isotopes in a saline Antarctic lake. *Geomicrobiol J* **1**: 329–340.

Buschmann, S., Warkentin, E., Xie, H., Langer, J.D., Ermler, U., and Michel, H. (2010) The structure of *cbb3* cytochrome oxidase provides insights into proton pumping. *Science* **329**: 327–330.

Calisto, F., and Pereira, M.M. (2021) The ion-translocating NrfD-like subunit of energy-transducing membrane complexes. *Front Chem* **9**: 663706.

Cavicchioli, R. (2015) Microbial ecology of Antarctic aquatic systems. *Nat Rev Microbiol* **13**: 691–706.

Chaumeil, P.-A., Mussig, A.J., Hugenholtz, P., and Parks, D.H. (2019) GTDB-Tk: a toolkit to classify genomes with the Genome Taxonomy Database. *Bioinformatics* **36**: 1925–1927.

Chuvochina, M., Rinke, C., Parks, D.H., Rappé, M.S., Tyson, G.W., Yilmaz, P., *et al*. (2019) The importance of designating type material for uncultured taxa. *Syst Appl Microbiol* **42**: 15–21.

Clark, M.A., and Barrett, E.L. (1987) The *phs* gene and hydrogen sulfide production by *Salmonella typhimurium*. *J Bacteriol* **169**: 2391–2397.

Coppi, M.V., O'Neil, R.A., Leang, C., Kaufmann, F., Methe, B.A., Nevin, K.P., *et al*. (2007) Involvement of *Geobacter sulfurreducens* SfrAB in acetate metabolism rather than intracellular, respiration-linked Fe(III) citrate reduction. *Microbiology* **153**: 3572–3585.

Craig, L., Forest, K.T., and Maier, B. (2019) Type IV pili: dynamics, biophysics and functional consequences. *Nat Rev* **17**: 429–440.

da Silva, S.M., Voordouw, J., Leitão, C., Martins, M., Voordouw, G., and Pereira, I.A.C. (2013) Function of formate dehydrogenases in *Desulfovibrio vulgaris* Hildenborough energy metabolism. *Microbiology* **159**: 1760–1769.

Daebeler, A., Herbold, C.W., Vierheilig, J., Sedlacek, C.J., Pjevac, P., Albertsen, M., *et al*. (2018) Cultivation and genomic analysis of "*Candidatus* Nitrosocaldus islandicus," an obligately thermophilic, ammonia-oxidizing thaumarchaeon from a hot spring biofilm in Graendalur Valley, Iceland. *Front Microbiol* **9**: 193.

Dahl, C., Franz, B., Hensen, D., Kesselheim, A., and Zigann, R. (2013) Sulfite oxidation in the purple sulfur bacterium *Allochromatium vinosum*: identification of SoeABC as a major player and relevance of SoxYZ in the process. *Microbiology* **159**: 2626–2638.

Duarte, A.G., Santos, A.A., and Pereira, I.A. (2016) Electron transfer between the QmoABC membrane complex and adenosine 5′-phosphosulfate reductase. *Biochim Biophys Acta* **1857**: 380–386.

Edgar, R.C. (2004) MUSCLE: a multiple sequence alignment method with reduced time and space complexity. *BMC Bioinformatics* **5**: 113.

Einsle, O., Messerschmidt, A., Stach, P., Bourenkov, G.P., Bartunik, H.D., Huber, R., and Kroneck, P.M.H. (1999) Structure of cytochrome *c* nitrite reductase. *Nature* **400**: 476–480.

Evans, J.C., Huddler, D.P., Hilgers, M.T., Romanchuk, G., Matthews, R.G., and Ludwig, M.L. (2004) Structures of the N-terminal modules imply large domain motions during catalysis by methionine synthase. *Proc Natl Acad Sci U S A* **101**: 3729–3736.

Foo, C.-Y., Pethe, K., and Lupien, A. (2020) Oxidative phosphorylation—an update on a new, essential target space for drug discovery in *Mycobacterium tuberculosis*. *Appl Sci* **10**: 2339.

Franzmann, P.D., Roberts, N.J., Mancuso, C.A., Burton, H. R., and McMeekin, T.A. (1991) Methane production in meromictic Ace Lake, Antarctica. *Hydrobiology* **210**: 191–201.

Frigaard, N.-U., and Bryant, D.A. (2008) Genomics insights into the sulfur metabolism of phototrophic green sulfur bacteria. In *Advances in Photosynthesis and Respiration*, Vol. **27**, Hell, R., Dahl, C., Knaff, D.B., and Leustek, T. (eds). Heidelberg: Springer, pp. 337–355.

Giltner, C.L., Nguyen, Y., and Burrows, L.L. (2012) Type IV pilin proteins: versatile molecular modules. *Microbiol Mol Biol Rev* **76**: 740–772.

Greening, C., Biswas, A., Carere, C.R., Jackson, C.J., Taylor, M.C., Stott, M.B., *et al*. (2016) Genomic and metagenomic surveys of hydrogenase distribution indicate H_2 is a widely utilised energy source for microbial growth and survival. *ISME J* **10**: 761–777.

Gregersen, L.H., Bryant, D.A., and Frigaard, N.-U. (2011) Mechanisms and evolution of oxidative sulfur metabolism in green sulfur bacteria. *Front Microbiol* **2**: 116.

Gristwood, T., McNeil, M.B., Clulow, J.S., Salmond, G.P., and Fineran, P.C. (2011) PigS and PigP regulate prodigiosin biosynthesis in *Serratia* via differential control

of divergent operons, which include predicted transporters of sulfur-containing molecules. *J Bacteriol* **193**: 1076–1085.

Heim, S., Kunkel, A., Thauer, R.K., and Hedderich, R. (1998) Thiol:fumarate reductase (Tfr) from *Methanobacterium thermoautotrophicum* – identification of the catalytic sites for fumarate reduction and thiol oxidation. *Eur J Biochem* **253**: 292–299.

Heinzinger, N.K., Fujimoto, S.Y., Clark, M.A., Moreno, M.S., and Barrett, E.L. (1995) Sequence analysis of the *phs* operon in *Salmonella typhimurium* and the contribution of thiosulfate reduction to anaerobic energy metabolism. *J Bacteriol* **177**: 2813–2820.

Herlemann, D.P.R., Geissinger, O., Ikeda-Ohtsubo, W., Kunin, V., Sun, H., Lapidus, A., *et al*. (2009) Genomic analysis of "*Elusimicrobium minutum*," the first cultivated representative of the phylum "Elusimicrobia" (formerly Termite Group 1). *Appl Environ Microbiol* **75**: 2841–2849.

Hinsley, A.P., and Berks, B.C. (2002) Specificity of respiratory pathways involved in the reduction of sulfur compounds by Salmonella enterica. *Microbiology* **148**: 3631–3638.

Hoang, D.T., Chernomor, O., von Haeseler, A., Minh, B.Q., and Vinh, L.S. (2017) UFBoot2: improving the ultrafast bootstrap approximation. *Mol Biol Evol* **35**: 518–522.

Holkenbrink, C., Ocón Barbas, S., Mellerup, A., Otaki, H., and Frigaard, N.-U. (2011) Sulfur globule oxidation in green sulfur bacteria is dependent on the dissimilatory sulfite reductase system. *Microbiology* **157**: 1229–1239.

Huntemann, M., Ivanova, N.N., Mavromatis, K., Tripp, H.J., Paez-Espino, D., Tennessen, K., *et al*. (2015) The standard operating procedure of the DOE-JGI Metagenome Annotation Pipeline (MAP v.4). *Stand Genomic Sci* **11**: 17.

Huson, D.H., and Scornavacca, C. (2012) Dendroscope 3: An interactive tool for rooted phylogenetic trees and networks. *Syst Biol* **61**: 1061–1067.

Jain, C., Rodriguez-R, L.M., Phillippy, A.M., Konstantinidis, K.T., Aluru, S., *et al*. (2018) High throughput ANI analysis of 90K prokaryotic genomes reveals clear species boundaries. *Nat Commun* **9**: 5114.

Jormakka, M., Yokoyama, K., Yano, T., Tamakoshi, M., Akimoto, S., Shimamura, T., *et al*. (2008) Molecular mechanism of energy conservation in polysulfide respiration. *Nat Struct Mol Biol* **15**: 730–737.

Kadnikov, V.V., Mardanov, A.V., Podosokorskaya, O.A., Gavrilov, S.N., Kublanov, I.V., Beletsky, A.V., *et al*. (2013) Genomic analysis of *Melioribacter roseus*, facultatively anaerobic organotrophic bacterium representing a novel deep lineage within Bacteriodetes/Chlorobi group. *PLoS One* **8**: e53047.

Kalyaanamoorthy, S., Minh, B.Q., Wong, T.K.F., von Haeseler, A., and Jermiin, L.S. (2017) ModelFinder: fast model selection for accurate phylogenetic estimates. *Nat Methods* **14**: 587–589.

Kang, D.D., Li, F., Kirton, E., Thomas, A., Egan, R., An, H., *et al*. (2019) MetaBAT 2: an adaptive binning algorithm for robust and efficient genome reconstruction from metagenome assemblies. *PeerJ* **7**: e7359.

Kashyap, D.R., Botero, L.M., Franck, W.L., Hassett, D.J., and McDermott, T.R. (2006) Complex regulation of arsenite oxidation in *Agrobacterium tumefaciens*. *J Bacteriol* **188**: 1081–1088.

Kaster, A.K., Moll, J., Parey, K., and Thauer, R.K. (2011) Coupling of ferredoxin and heterodisulfide reduction via electron bifurcation in hydrogenotrophic methanogenic archaea. *Proc Natl Acad Sci U S A* **108**: 2981–2986.

Kaufmann, F., and Lovley, D.R. (2001) Isolation and characterization of a soluble NADPH-dependent Fe(III) reductase from *Geobacter sulfurreducens*. *J Bacteriol* **183**: 4468–4476.

Kemp, R.G., and Tripathi, R.L. (1993) Pyrophosphate-dependent phosphofructo-1-kinase complements fructose 1,6-bisphosphatase but not phosphofructokinase deficiency in *Escherichia coli*. *J Bacteriol* **175**: 5723–5724.

Kennedy, N.W., Mills, C.E., Nichols, T.M., Abrahamson, C. H., and Tullman-Ercek, D. (2021) Bacterial microcompartments: tiny organelles with big potential. *Curr Opin Microbiol* **63**: 36–42.

Kerby, R.L., Hong, S.S., Ensign, S.A., Coppoc, L.J., Ludden, P.W., and Roberts, G.P. (1992) Genetic and physiological characterization of the *Rhodospirillum rubrum* carbon monoxide dehydrogenase system. *J Bacteriol* **174**: 5284–5294.

Kertesz, M.A. (1999) Riding the sulfur cycle – metabolism of sulfonates and sulfate esters in Gram-negative bacteria. *FEMS Microbiol Rev* **24**: 135–175.

Konstantinidis, K.T., Rosselló-Móra, R., and Amann, R. (2017) Uncultivated microbes in need of their own taxonomy. *ISME J* **11**: 2399–2406.

Krafft, T., Bokranz, M., Klimmek, O., Schröder, I., Fahrenholz, F., Kojro, E., *et al*. (1992) Cloning and nucleotide sequence of the *psrA* gene of *Wolinella succinogenes* polysulphide reductase. *Eur J Biochem* **206**: 503–510.

Kublanov, I.V., Sigalova, O.M., Gavrilov, S.N., Lebedinsky, A.V., Rinke, C., Kovaleva, O., *et al*. (2017) Genomic analysis of *Caldithrix abyssi*, the thermophilic anaerobic bacterium of the novel bacterial phylum Caldithrichaeota. *Front Microbiol* **8**: 195.

Kumar, S., Stecher, G., Li, M., Knyaz, C., and Tamura, K. (2018) MEGA X: molecular evolutionary genetics analysis across computing platforms. *Mol Biol Evol* **35**: 1547–1549.

Lauro, F.M., DeMaere, M.Z., Yau, S., Brown, M.V., Ng, C., Wilkins, D., *et al*. (2011) An integrative study of a meromictic lake ecosystem in Antarctica. *ISME J* **5**: 879–895.

Levin, B.J., Huang, Y.Y., Peck, S.C., Wei, Y., Martinez-Del Campo, A., Marks, J.A., *et al*. (2017) A prominent glycyl radical enzyme in human gut microbiomes metabolizes *trans*-4-hydroxy-L-proline. *Science* **355**: 1–28.

Li, D., Luo, R., Liu, C.M., Leung, C.M., Ting, H.F., Sadakane, K., *et al*. (2016) MEGAHIT v1.0: a fast and scalable metagenome assembler driven by advanced methodologies and community practices. *Methods* **102**: 3–11.

Li, F., Hagemeier, C.H., Seedorf, H., Gottschalk, G., and Thauer, R.K. (2007) *Re*-citrate synthase from *Clostridium kluyveri* is phylogenetically related to homocitrate synthase and isopropylmalate synthase rather than to *Si*-citrate synthase. *J Bacteriol* **189**: 4299–4304.

Liu, L., Wang, Y., Che, Y., Chen, Y., Xia, Y., Luo, R., *et al.* (2020). High-quality bacterial genomes of a partial-

nitritation/anammox system by an iterative hybrid assembly method. *Microbiome* **8**: 155.
Lledo, B., Martinez-Espinosa, R.M., Marhuenda-Egea, F.C., and Bonete, M.J. (2004) Respiratory nitrate reductase from haloarchaeon *Haloferax mediterranei*: biochemical and genetic analysis. *Biochim Biophys Acta* **1674**: 50–59.
Lombard, V., Golaconda Ramulu, H., Drula, E., Coutinho, P. M., and Henrissat, B. (2014) The carbohydrate-active enzymes database (CAZy) in 2013. *Nucleic Acids Res* **42**: D490–D495.
Loosmore, S.M., Shortreed, J.M., Coleman, D.C., England, D.M., and Klein, M.H. (1996) Sequences of the genes encoding the A, B and C subunits of the *Haemophilus influenzae* dimethylsulfoxide reductase complex. *Gene* **169**: 137–138.
Lu, Z., and Imlay, J.A. (2017) The fumarate reductase of *Bacteroides thetaiotaomicron*, unlike that of *Escherichia coli*, is configured so that it does not generate reactive oxygen species. *mBio* **8**: e01873-16.
Ma, K., Schicho, R.N., Kelly, R.M., and Adams, M.W.W. (1993) Hydrogenase of the hyperthermophilic *Pyrococcus furiosus* is an elemental sulfur reductase or sulfhydrogenase: evidence for a sulfur-reducing hydrogenase ancestor. *Proc Natl Acad Sci U S A* **90**: 5341–5344.
Ma, K., Weiss, R., and Adams, M.W.W. (2000) Characterization of hydrogenase II from the hyperthermophilic archaeon *Pyrococcus furiosus* and assessment of its role in sulfur reduction. *J Bacteriol* **182**: 1864–1871.
Mai, X., and Adams, M.W.W. (1994) Indolepyruvate ferredoxin oxidoreductase from the hyperthermophilic archaeon *Pyrococcus furiosus*. *J Biol Chem* **269**: 16726–16732.
Maini Rekdal, V., Bess, E.N., Bisanz, J.E., Turnbaugh, P.J., and Balskus, E.P. (2019) Discovery and inhibition of an interspecies gut bacterial pathway for levodopa metabolism. *Science* **364**: eaau6323.
Malasarn, D., Saltikov, C.W., Campbell, K.M., Santini, J.M., Hering, J.G., and Newman, D.K. (2004) *arrA* is a reliable marker for As(V) respiration. *Science* **306**: 455.
Marco-Urrea, E., Paul, S., Khodaverdi, V., Seifert, J., von Bergen, M., Kretzschmar, U., *et al*. (2011) Identification and characterization of a *Re*-citrate synthase in *Dehalococcoides* strain CBDB1. *J Bacteriol* **193**: 5171–5178.
Marnocha, C.L., Levy, A.T., Powell, D.H., Hanson, T.E., and Chan, C.S. (2016) Mechanisms of extracellular S_0 globule production and degradation in *Chlorobaculum tepidum* via dynamic cell-globule interactions. *Microbiology* **162**: 1125–1134.
Marreiros, B.C., Calisto, F., Castro, P.J., Duarte, A.M., Sena, F. V., Silva, A.F., *et al*. (2016) Exploring membrane respiratory chains. *Biochim Biophys Acta* **1857**: 1039–1067.
Matheus Carnevali, P.B., Schulz, F., Castelle, C.J., Kantor, R.S., Shih, P.M., Sharon, I., *et al*. (2019) Hydrogen-based metabolism as an ancestral trait in lineages sibling to the Cyanobacteria. *Nat Commun* **10**: 463.
Mayer, F., and Müller, V. (2014) Adaptations of anaerobic archaea to life under extreme energy limitation. *FEMS Microbiol Rev* **38**: 449–472.
Méheust, R., Castelle, C.J., Carnevali, P.B.M., Farag, I.F., He, C., Chen, L.X., *et al*. (2020) Groundwater *Elusimicrobia* are metabolically diverse compared to gut microbiome *Elusimicrobia* and some have a novel nitrogenase paralog. *ISME J* **14**: 2907–2922.
Mertens, E. (1991) Pyrophosphate-dependent phosphofructokinase, an anaerobic glycolytic enzyme? *FEBS Lett* **285**: 1–5.
Momper, L., Jungbluth, S.P., Lee, M.D., and Amend, J.P. (2017) Energy and carbon metabolisms in a deep terrestrial subsurface fluid microbial community. *ISME J* **11**: 2319–2333.
Momper, L.M., Casar, C.P., and Osburn, M.R. (2021) A metagenomic view of novel microbial and metabolic diversity found within the deep terrestrial biosphere. *bioRxiv*.
Muller, J.A., and DasSarma, S. (2005) Genomic analysis of anaerobic respiration in the archaeon *Halobacterium* sp. strain NRC-1: dimethyl sulfoxide and trimethylamine N-oxide as terminal electron acceptors. *J Bacteriol* **187**: 1659–1667.
Murray, A.E., Freudenstein, J., Gribaldo, S., Hatzenpichler, R., Hugenholtz, P., Kämpfer, P., *et al*. (2020) Roadmap for naming uncultivated archaea and bacteria. *Nat Microbiol* **5**: 987–994.
Nayfach, S., Roux, S., Seshadri, R., Udwary, D., Varghese, N., Schulz, F., *et al*. (2020) A genomic catalog of Earth's microbiomes. *Nat Biotechnol* **39**: 499–509.
Ng, S.C., De Maere, M., Williams, T.J., Lauro, F.M., Raftery, M.J., Gibson, J., *et al*. (2010) Metaproteogenomic analysis of a dominant green sulfur bacterium from Ace Lake, Antarctica. *ISME J* **4**: 1002–1019.
Nguyen, L.-T., Schmidt, H.A., von Haeseler, A., and Minh, B. Q. (2015) IQ-TREE: a fast and effective stochastic algorithm for estimating maximum likelihood phylogenies. *Mol Biol Evol* **32**: 268–274.
Nunoura, T., Chikaraishi, Y., Izaki, R., Suwa, T., Sato, T., Harada, T., *et al*. (2018) A primordial and reversible TCA cycle in a facultatively chemolithoautotrophic thermophile. *Science* **359**: 559–563.
Ogawa, K., Akagawa, E., Yamane, K., Sun, Z.W., LaCelle, M., Zuber, P., *et al*. (1995) The *nasB* operon and *nasA* gene are required for nitrate/nitrite assimilation in *Bacillus subtilis*. *J Bacteriol* **177**: 1409–1413.
Orellana, L.H., Francis, T.B., Ferraro, M., Hehemann, J.H., Fuchs, B.M., and Amann, R.I. (2021) Verrucomicrobiota are specialist consumers of sulfated methyl pentoses during diatom blooms. *ISME J* **16**: 630–641. https://doi.org/10.1038/s41396-021-01105-7.
Ortiz, M., Leung, P.M., Shelley, G., Jirapanjawat, T., Nauer, P.A., Van Goethem, M.W., *et al*. (2021) Multiple energy sources and metabolic strategies sustain microbial diversity in Antarctic desert soils. *Proc Natl Acad Sci U S A* **118**: e2025322118.
Panwar, P., Allen, M.A., Williams, T.J., Hancock, A.M., Brazendale, S., Bevington, J., *et al*. (2020) Influence of the polar light cycle on seasonal dynamics of an Antarctic lake microbial community. *Microbiome* **8**: 116.
Panwar, P., Allen, M.A., Williams, T.J., Haque, S., Brazendale, S., Hancock, A.M., *et al*. (2021) Remarkably coherent population structure for a dominant Antarctic *Chlorobium* species. *Microbiome* **9**: 231.
Parks, D.H., Chuvochina, M., Chaumeil, P.-A., Rinke, C., Mussig, A.J., and Hugenholtz, P. (2020) A complete

domain-to-species taxonomy for bacteria and archaea. *Nat Biotechnol* **38**: 1079–1086.

Parks, D.H., Imelfort, M., Skennerton, C.T., Hugenholtz, P., and Tyson, G.W. (2015) CheckM: assessing the quality of microbial genomes recovered from isolates, single cells, and metagenomes. *Genome Res* **25**: 1043–1055.

Parks, D.H., Rinke, C., Chuvochina, M., Chaumeil, P.-A., Woodcroft, B.J., Evans, P.N., *et al*. (2017) Recovery of nearly 8,000 metagenome-assembled genomes substantially expands the tree of life. *Nat Microbiol* **2**: 1533–1542.

Pearson, W.R. (2013) Chapter 3: Unit 3.1: An introduction to sequence similarity ("homology") searching. In *Current Protocols in Bioinformatics*. Hoboken, NJ: John Wiley & Sons, Inc.

Poudel, S., Tokmina-Lukaszewska, M., Colman, D.R., Refai, M., Schut, G.J., King, P.W., *et al*. (2016) Unification of [FeFe]-hydrogenases into three structural and functional groups. *Biochim Biophys Acta* **1860**: 1910–1921.

Ragsdale, S.W., and Pierce, E. (2008) Acetogenesis and the Wood-Ljungdahl pathway of CO_2 fixation. *Biochim Biophys Acta* **1784**: 1873–1898.

Rankin, L.M., Gibson, J.A.E., Franzmann, P.D., and Burton, H.R. (1999) The chemical stratification and microbial communities of Ace Lake, Antarctica: a review of the characteristics of a marine-derived meromictic lake. *Polarforschung* **66**: 33–52.

Rehm, B.H.A. (2010) Bacterial polymers: biosynthesis, modifications and applications. *Nat Rev Microbiol* **8**: 578–592.

Reisky, L., Préchoux, A., Zühlke, M.K., Bäumgen, M., Robb, C.S., Gerlach, N., *et al*. (2019) A marine bacterial enzymatic cascade degrades the algal polysaccharide ulvan. *Nat Chem Biol* **15**: 803–812.

Rinke, C., Schwientek, P., Sczyrba, A., Ivanova, N.N., Anderson, I.J., Cheng, J.-F., *et al*. (2013) Insights into the phylogeny and coding potential of microbial dark matter. *Nature* **499**: 431–437.

Rosner, B.M., and Schink, B. (1995) Purification and characterization of acetylene hydratase of *Pelobacter acetylenicus*, a tungsten iron-sulfur protein. *J Bacteriol* **177**: 5767–5772.

Saltikov, C.W., and Newman, D.K. (2003) Genetic identification of a respiratory arsenate reductase. *Proc Natl Acad Sci U S A* **100**: 10983–10988.

Santini, J.M., and vanden Hoven, R.N. (2004) Molybdenum-containing arsenite oxidase of the chemolithoautotrophic arsenite oxidizer NT-26. *J Bacteriol* **186**: 1614–1619.

Sapra, R., Bagramyan, K., and Adams, M.W.W. (2003) A simple energy-conserving system: proton reduction coupled to proton translocation. *Proc Natl Acad Sci U S A* **100**: 7545–7550.

Schoelmerich, M.C., and Müller, V. (2019) Energy conservation by a hydrogenase-dependent chemiosmotic mechanism in an ancient metabolic pathway. *Proc Natl Acad Sci U S A* **116**: 6329–6334.

Schoepp-Cothenet, B., van Lis, R., Philippot, P., Magalon, A., Russell, M.J., and Nitschke, W. (2012) The ineluctable requirement for the trans-iron elements molybdenum and/or tungsten in the origin of life. *Sci Rep* **2**: 263.

Schröder, I., Rech, S., Krafft, T., and Macy, J.M. (1997) Purification and characterization of the selenate reductase from *Thauera selenatis*. *J Biol Chem* **272**: 23765–23768.

Schuchmann, K., and Müller, V. (2016) Energetics and application of heterotrophy in acetogenic bacteria. *Appl Environ Microbiol* **82**: 4056–4069.

Schut, G.J., Zhou, J., and Adam, M.W.W. (2001) DNA microarray analysis of the hyperthermophilic archaeon *Pyrococcus furiosus*: evidence for a new type of sulfur-reducing enzyme complex. *J Bacteriol* **183**: 7027–7036.

Shuber, A.P., Orr, E.C., Recny, M.A., Schendel, P.F., May, H.D., Schauer, N.L., and Ferry, J.G. (1986) Cloning, expression, and nucleotide sequence of the formate dehydrogenase genes from *Methanobacterium formicicum*. *J Biol Chem* **261**: 12942–12947.

Silva, P.J., de Castro, B., and Hagen, W.R. (1999) On the prosthetic groups of the NiFe sulfhydrogenase from *Pyrococcus furiosus*: topology, structure, and temperature-dependent redox chemistry. *J Biol Inorg Chem* **4**: 284–291.

Simon, J., and Kroneck, P.M. (2013) Microbial sulfite respiration. *Adv Microb Physiol* **62**: 45–117.

Singer, S.W., Hirst, M.B., and Ludden, P.W. (2006) CO-dependent H_2 evolution by *Rhodospirillum rubrum*: role of CODH:CooF complex. *Biochim Biophys Acta* **1757**: 1582–1591.

Søndergaard, D., Pedersen, C.N.S., and Greening, C. (2016) HydDB: a web tool for hydrogenase classification and analysis. *Sci Rep* **6**: 34212.

Stoffels, L., Krehenbrink, M., Berks, B.C., and Unden, G. (2012) Thiosulfate reduction in *Salmonella enterica* is driven by the proton motive force. *J Bacteriol* **194**: 475–485.

Sutter, M., Melnicki, M.R., Schulz, F., Woyke, T., and Kerfeld, C.A. (2021) A catalog of the diversity and ubiquity of bacterial microcompartments. *Nat Commun* **12**: 3809.

Tanaka, Y., Yoshikaie, K., Takeuchi, A., Ichikawa, M., Mori, T., Uchino, S., *et al*. (2020) Crystal structure of a YeeE/YedE family protein engaged in thiosulfate uptake. *Sci Adv* **6**: eaba7637.

Thorell, H.D., Stenklo, K., Karlsson, J., and Nilsson, T. (2003) A gene cluster for chlorate metabolism in *Ideonella dechloratans*. *Appl Environ Microbiol* **69**: 5585–5592.

Ticak, T., Kountz, D.J., Girosky, K.E., Krzycki, J.A., and Ferguson, D.J., Jr. (2014) A nonpyrrolysine member of the widely distributed trimethylamine methyltransferase family is a glycine betaine methyltransferase. *Proc Natl Acad Sci U S A* **111**: E4668–E4676.

Tremblay, P.L., Zhang, T., Dar, S.A., Leang, C., and Lovley, D.R. (2013) The Rnf complex of *Clostridium ljungdahlii* is a proton-translocating ferredoxin:NAD^+ oxidoreductase essential for autotrophic growth. *mBio* **4**: E00406–E00412.

Trüper, H.G., and Euzéby, J.P. (2009) International code of nomenclature of prokaryotes. Appendix 9: orthography. *Int J Syst Evol Microbiol* **59**: 2107–2113.

Ulmer, J.E., Vilén, E.M., Namburi, R.B., Benjdia, A., Beneteau, J., Malleron, A., *et al*. (2014) Characterization of glycosaminoglycan (GAG) sulfatases from the human gut symbiont *Bacteroides thetaiotaomicron* reveals the first GAG-specific bacterial endosulfatase. *J Biol Chem* **289**: 24289–24303.

van Vliet, D.M., Palakawong, N., Ayudthaya, S., Diop, S., Villanueva, L., Stams, A.J.M., and Sánchez-Andrea, I. (2019) Anaerobic degradation of sulfated polysaccharides by two novel Kiritimatiellales strains isolated from Black Sea sediment. *Front Microbiol* **10**: 253.

Varga, M.E., and Weiner, J.H. (1995) Physiological role of GlpB of anaerobic glycerol-3-phosphate dehydrogenase of *Escherichia coli*. *Biochem Cell Biol* **73**: 147–153.

Venceslau, S.S., Lino, R.R., and Pereira, I.A. (2010) The Qrc membrane complex, related to the alternative complex III, is a menaquinone reductase involved in sulfate respiration. *J Biol Chem* **285**: 22774–22783.

Venugopal, A., Bryk, R., Shi, S., Rhee, K., Rath, P., Schnappinger, D., *et al*. (2011) Virulence of *Mycobacterium tuberculosis* depends on lipoamide dehydrogenase, a member of three multienzyme complexes. *Cell Host Microbe* **9**: 21–31.

Walsby, A.E. (1994) Gas vesicles. *Microbiol Rev* **58**: 94–144.

Wegner, C.-E., Richter-Heitmann, T., Klindworth, A., Klockow, C., Richter, M., Achstetter, T., *et al*. (2013) Expression of sulfatases in *Rhodopirellula baltica* and the diversity of sulfatases in the genus *Rhodopirellula*. *Mar Genomics* **9**: 51–61.

Weiner, J.H., MacIsaac, D.P., Bishop, R.E., and Bilous, P.T. (1988) Purification and properties of *Escherichia coli* dimethyl sulfoxide reductase, an iron-sulfur molybdoenzyme with broad substrate specificity. *J Bacteriol* **170**: 1505–1510.

Williams, T.J., Allen, M.A., Berengut, J.F., and Cavicchioli, R. (2021a) Shedding light on microbial "dark matter": insights into novel Cloacimonadota and Omnitrophota from an Antarctic lake. *Front Microbiol* **12**: 741077.

Williams, T.J., Allen, M.A., Ivanova, N., Huntemann, M., Haque, S., Hancock, A.M., *et al*. (2021b) Genome analysis of a verrucomicrobial endosymbiont with a tiny genome discovered in an Antarctic lake. *Front Microbiol* **12**: 674758.

Winter, S.E., Thiennimitr, P., Winter, M.G., Butler, B.P., Huseby, D.L., Crawford, R.W., *et al*. (2010) Gut inflammation provides a respiratory electron acceptor for *Salmonella*. *Nature* **467**: 426–429.

Wood, A.P., Aurikko, J.P., and Kelly, D.P. (2004) A challenge for 21st century molecular biology and biochemistry: what are the causes of obligate autotrophy and methanotrophy? *FEMS Microbiol Rev* **28**: 335–352.

Youssef, N.H., Farag, I.F., Hahn, C.R., Jarrett, J., Becraft, E., Eloe-Fadrosh, E., *et al*. (2019a) Genomic characterization of candidate division LCP-89 reveals an atypical cell wall structure, microcompartment production, and dual respiratory and fermentative capacities. *Appl Environ Microbiol* **85**: e00110-19.

Youssef, N.H., Farag, I.F., Rinke, C., Hallam, S.J., Woyke, T., and Elshahed, M.S. (2015) *In silico* analysis of the metabolic potential and niche specialization of candidate phylum "Latescibacteria" (WS3). *PLoS One* **10**: e0127499.

Youssef, N.H., Farag, I.F., Rudy, S., Mulliner, A., Walker, K., Caldwell, F., *et al*. (2019b) The Wood–Ljungdahl pathway as a key component of metabolic versatility in candidate phylum Bipolaricaulota (Acetothermia, OP1). *Environ Microbiol Rep* **11**: 538–547.

Yu, H., Wu, C.H., Schut, G.J., Haja, D.K., Zhao, G., Peters, J.W., *et al*. (2018) Structure of an ancient respiratory system. *Cell* **173**: 1636–1649.

Zamkovaya, T., Foster, J.S., de Crécy-Lagard, V., and Conesa, A. (2021) A network approach to elucidate and prioritize microbial dark matter in microbial communities. *ISME J* **15**: 228–244.

Zangelmi, E., Stanković, T., Malatesta, M., Acquotti, D., Pallitsch, K., and Peracchi, A. (2021) Discovery of a new, recurrent enzyme in bacterial phosphonate degradation: (R)-1-Hydroxy-2-aminoethylphosphonate ammonia-lyase. *Biochemistry* **60**: 1214–1225.

Zhuang, W.-Q., Yi, S., Bill, M., Brisson, V.L., Feng, X., Men, Y., *et al*. (2014) Incomplete Wood–Ljungdahl pathway facilitates one-carbon metabolism in organohalide-respiring *Dehalococcoides mccartyi*. *Proc Natl Acad Sci U S A* **111**: 6419–6424.

Supporting Information

Additional Supporting Information may be found in the online version of this article at the publisher's web-site:

Appendix S1. Other sulfur metabolism enzymes.

Fig, S1. Sulfate and sulfide concentrations in Ace Lake.

Fig. **S2**. Maximum-likelihood tree of corrinoid:methyltransferases from select Ace Lake metagenome-assembled genomes and reference sequences.

Fig. **S3**. Methionine synthase gene cluster arrangement.

Fig. **S4**. Normalized coverage data for selected sulfur cycling enzymes across different depths and seasons in Ace Lake, shown in logarithmic scale.

Table S4. Proteins homologous to methionine synthase domains, and a novel methyltransferase encoded in the same gene cluster.

Table S1. Proteins and Gene IDs for Ace Lake MAGs and SURF_26 chosen for analysis in this study. (Excel spread sheet)

Table S2. Etymologies and metadata for proposed new *Candidatus* genus and species. (Excel spread sheet)

Table S3. MAG abundance data. (Excel spread sheet)